AD-A031 519 LITTON SYSTEMS INC WOODLAND HILLS CALIF GUIDANCE AND--ETC F/G 17/7
NO-DROP WEAPON SCORING STUDY.(U)
AUG 76 J S AUSMAN N00173-76-C-0247
UNCLASSIFIED G/CSD-403343 NRL-76-001 NL

1 OF 1
ADA031519

END
DATE FILMED
12 - 76

UNCLASSIFIED

SECURITY CLASSIFICATION OF THIS PAGE (When Data Entered)

REPORT DOCUMENTATION PAGE		READ INSTRUCTIONS BEFORE COMPLETING FORM
1. REPORT NUMBER USNRL-76-001	2. GOVT ACCESSION NO.	3. RECIPIENT'S CATALOG NUMBER
4. TITLE (and Subtitle) NO-DROP WEAPON SCORING STUDY.		5. TYPE OF REPORT & PERIOD COVERED Final Report.
		6. PERFORMING ORG. REPORT NUMBER 403343
7. AUTHOR(s) J.S. Ausman		8. CONTRACT OR GRANT NUMBER(s) N00173-76-C-0247
9. PERFORMING ORGANIZATION NAME AND ADDRESS Litton Guidance & Control Systems Div 5500 Canoga Avenue Woodland Hills, California		10. PROGRAM ELEMENT, PROJECT, TASK AREA & WORK UNIT NUMBERS WUC 401044
11. CONTROLLING OFFICE NAME AND ADDRESS U.S. Naval Research Laboratory Washington, D.C. 20375		12. REPORT DATE August 1976 13. NUMBER OF PAGES 68
14. MONITORING AGENCY NAME & ADDRESS(if different from Controlling Office) G/CSD-403343		15. SECURITY CLASS. (of this report) UNCLASSIFIED 15a. DECLASSIFICATION/DOWNGRADING SCHEDULE

16. DISTRIBUTION STATEMENT (of this Report)

DISTRIBUTION STATEMENT A
Approved for public release;
Distribution Unlimited

12 65p.

17. DISTRIBUTION STATEMENT (of the abstract entered in Block 20, if different from Report)

18 NRL 19 76-001

18. SUPPLEMENTARY NOTES

DDC
RECEIVED
NOV 2 1976
A

19. KEY WORDS (Continue on reverse side if necessary and identify by block number)

20. ABSTRACT (Continue on reverse side if necessary and identify by block number)

This report summarizes the results of a No-Drop Weapon Scoring (NDWS) study performed by Litton Guidance and Control Systems. The report contains a description of the impact prediction process and its accuracy in terms of sensitivities to measurement errors. Setting these impact prediction errors equal to the expected ballistic dispersion yields a set of acceptable measurement error tolerances. The study discusses mechanization of an NDWS to obtain these measurement accuracies. A summary description of an Airborne Range Instrumentation System (ARIS), along with flight test results, is included as an example of satisfactory mechanization.

DD FORM 1 JAN 73 1473 EDITION OF 1 NOV 65 IS OBSOLETE

UNCLASSIFIED 401044

SECURITY CLASSIFICATION OF THIS PAGE (When Data Entered)

LB

SECURITY CLASSIFICATION OF THIS PAGE(When Data Entered)

SECURITY CLASSIFICATION OF THIS PAGE(When Data Entered)

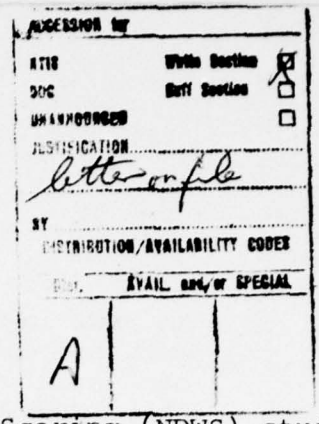

SUMMARY

This is the final report of a No-Drop Weapon Scoring (NDWS) study performed by Litton Guidance and Control Systems for the U.S. Navy under Contract No. N00173-76-C-0247. The report contains a description of the impact prediction process and its accuracy in terms of sensitivities to measurement errors. Setting the resulting impact prediction errors equal to the expected ballistic dispersion of the simulated weapons yields a set of acceptable measurement error tolerances.

The study then addresses the question of mechanizing an NDWS to obtain these measurement accuracies. In particular, the general process of combining ground-based position tracking data with airborne-sensed acceleration data is studied. A summary description of an Airborne Range Instrumentation System (ARIS) is included, along with flight test results, as a real-world example of that which can be and has been done with a DME-inertial no-drop bomb scoring mechanization. A later section of the study is devoted to a comparison of relative costs between a radar-inertial and a DME-inertial no-drop weapon scoring range.

The major conclusions to be drawn from this study are summarized below:

1. Measurements of aircraft states at the release point for no-drop weapon scoring should be at least as accurate as the following:

Position	20 feet (horizontal) 30 feet (vertical)
Velocity	2 ft/sec (horizontal) 3 ft/sec (vertical)
Heading.	0.3 degrees
Roll Rate.	6 degrees/second
True Airspeed.	5 feet/second
Air Pressure and Temperature.	1 percent

2. To incorporate strafe scoring into NDWS would require position measurements accurate to 3 feet and pitch and heading measurements accurate to 0.1 degree.

3. An NDWS implemented with airborne inertial platform data combined with either DME or radar position tracking data can satisfy the above bomb scoring requirements comfortably, and may even satisfy the strafe scoring requirements.

4. ARIS, an existing DME-inertial no-drop bomb scoring system, has demonstrated that it possesses the accuracy, mobility, and operational versatility to score properly all-weather no-drop bombing runs which employ realistic tactics against unfamiliar (off range) targets.

5. A DME-inertial NDWS range will be less costly to acquire, maintain, and operate than will a radar-inertial NDWS of equivalent accuracy.

TABLE OF CONTENTS

TABLE OF CONTENTS (cont)

LIST OF ILLUSTRATIONS

LIST OF TABLES

SECTION I

INTRODUCTION

No Drop Weapon Scoring (NDWS) is the process of measuring the state vector (especially position, velocity, and attitude) of an aircraft at the instant of simulated weapon release and then using these data as initial conditions in solving the ballistic equations of motion to calculate the point at which the weapon would have impacted had one actually been released. Among the numerous factors which have combined in recent years to stimulate interest in such systems are:

a. Obsolescence of the tracking and scoring radars currently employed on training ranges.

b. Improved accuracy of modern digital airborne weapon delivery systems, which now are more accurate than the obsolete scoring systems.

c. Land use, ecology, and public safety objections to bomb dropping ranges.

d. Desire among operational tactical air squadrons for more realistic (off range) training exercises.

e. Increased operational costs which place a premium on efficient use of available training time.

As a result of this surge of interest, CNO tasked NAVAIR in June 1975 to develop a program to modernize the NDWS systems deployed on Navy training ranges. To implement this task, the Navy contracted with Litton (in June 1976) to apply its experience to the NDWS problem. Litton had developed a modern no-drop bomb scoring system known as ARIS (Airborne Range Instrumentation System) in 1973-74 (Reference 1) as the primary instrumentation system for the DDR&E radar bombing evaluation (RABVAL) program. This program was concluded successfully in 1975.

This final report documents the effort by Litton on the Navy contract. The report contains, initially, a description of the method employed by ARIS to calculate weapon impact points. This discussion details the exact quantities which must be known or measured in order to carry out the impact prediction calculation. A subsequent section presents derivations of the impact error sensitivities to each of these measurements, and converts these sensitivities into a set of measurement tolerances.

Having developed a set of rational measurement error tolerance specifications, the question of implementing or mechanizing a system to achieve these specifications is addressed, using various levels of accuracy of combined position tracking and airborne-sensed acceleration data. Of these generic types, the distance measuring equipment (DME) position sensor combined with an inertial acceleration sensor represents the most accurate all-weather system. The ARIS is such a system. For ready reference, Section IV includes a short description of ARIS and its flight test results, as obtained during the RABVAL program.

The final section of this report presents criteria for evaluating the relative cost of alternative NDWS system configurations. An illustrative example of the use of this method indicates that the advanced ARIS-type system is not only more accurate but is less expensive than an augmented radar-type system.

SECTION II
IMPACT PREDICTION

2.1 GENERAL

Figure 1 diagrams the overall impact prediction procedure, as employed on the ARIS no-drop bomb scoring system. It smooths aircraft position and velocity as measured both before and after the release point in order to obtain the most accurate estimate of the aircraft state vector at release. Bomb lever arm and ejection velocity corrections then modify the release point aircraft state vector to obtain the initial conditions of the bomb at the start of its ballistic trajectory. The horizontal components of this initial state vector enter the impact equation computation directly. The vertical components and true airspeed become inputs to the ballistic trajectory computation which calculates time-of-fall and trail for the impact point computation. Coriolis corrections complete the computation of the impact point.

A useful piece of auxilliary information is the accuracy (i.e., expected standard deviation) of the computed impact point. ARIS computes the standard deviation of the downrange and crossrange impact point coordinates based on the self-calculated covariance of the release point state vector and the impact sensitivities to initial condition errors.

2.2 IMPACT PREDICTION EQUATIONS

Figure 2 is a vector diagram illustrating the classical air/wind/ground velocity vector triangle. In this figure, however, the time-of-fall (t_f) multiplier converts each leg of the triangle from a velocity vector into a distance vector. In particular, the $V_g t_f$ vector represents the distance traveled by the aircraft (if it continued in unaccelerated flight after releasing the bomb) during the free fall flight time of the bomb.

If the bomb had zero drag, it would impact directly beneath the aircraft at the end of the $V_g t_f$ vector. Because of air drag, however, the bomb actually lands behind the aircraft by an amount T_R, the bomb trail. Bomb drag acts in direct opposition to the air velocity vector V_a and causes the trail vector to be parallel to the negative of the $V_a t_f$ vector. From the release point (X_R, Y_R), the impact point (X_I, Y_I) can be computed by

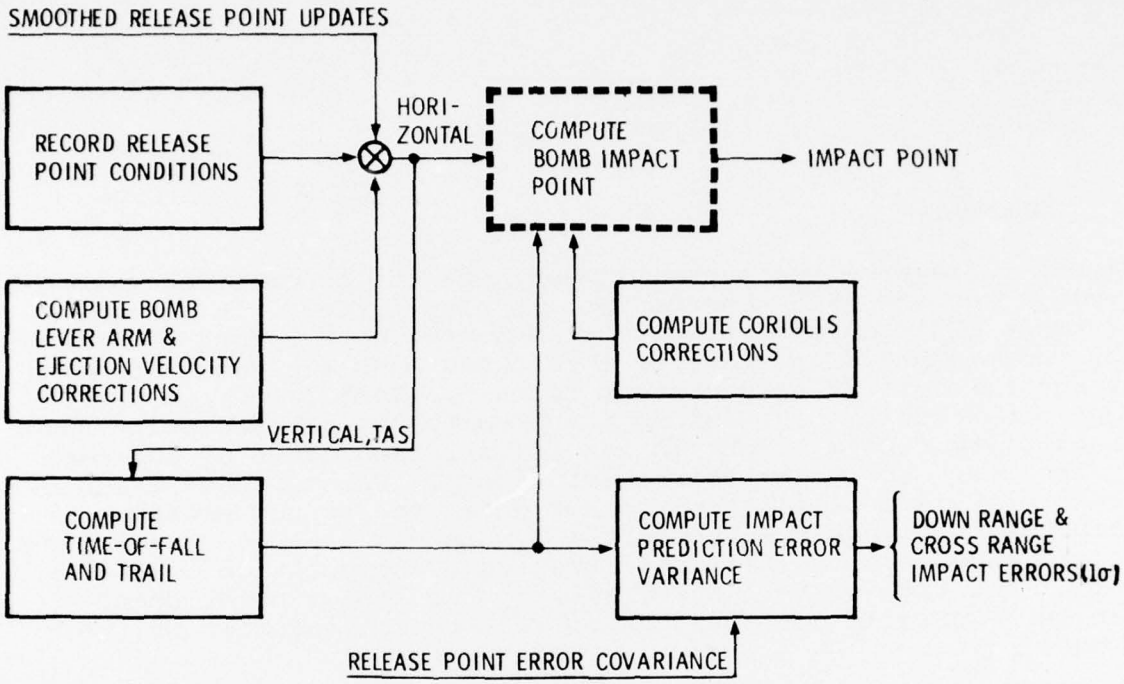

Figure 1. Impact Predictions

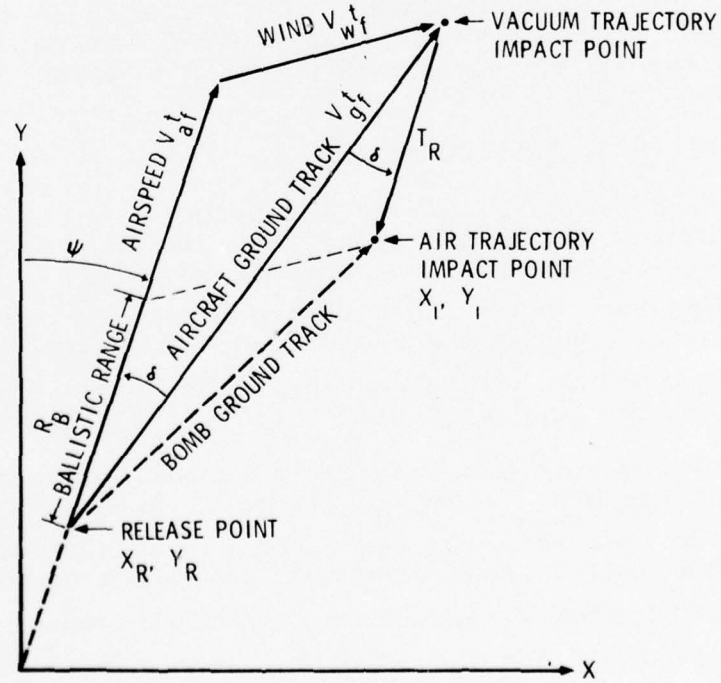

Figure 2. Geometry of Bomb Impact Predictions

multiplying ground velocity (V_g) by time-of-fall (t_f) and then subtracting trail (T_R) along the direction of the air velocity which, except for side slip angle, is equivalent to aircraft heading. Figure 3 describes this computational procedure in mathematical terms. The basic vector equation (release position plus ground velocity times time-of-fall minus trail along aircraft heading) is the same as that presented in figure 2.

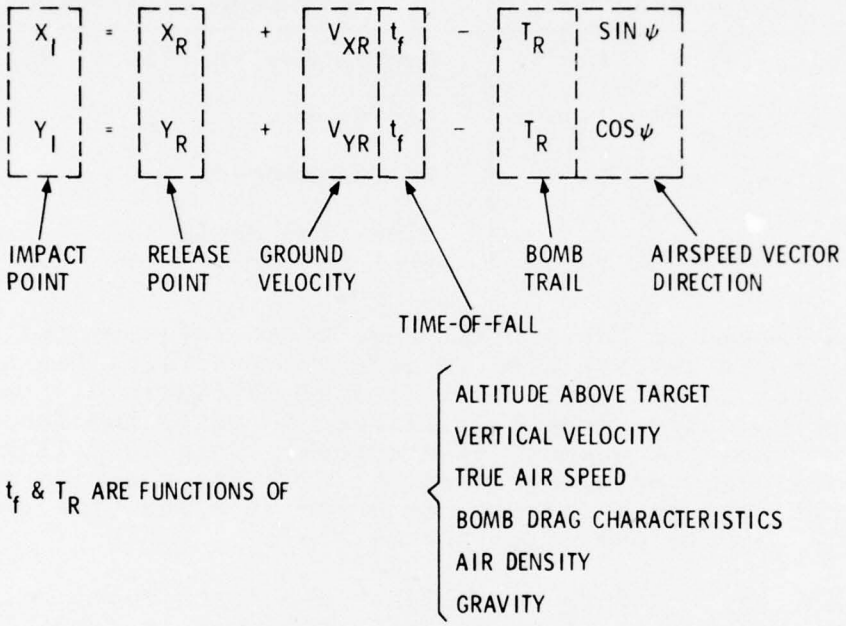

Figure 3. Basic Impact Prediction Equations

In mechanizing this equation, the NDWS must measure aircraft position, velocity, and heading at release. These are then modified slightly to account for bomb lever arm, aircraft attitude rate, release delay time, and ejection velocity effects to determine the position and velocity of the bomb at release. Bomb time-of-fall and trail are then computed by integrating the ballistic equations of motion. The subsequent sections discuss these steps in more detail.

2.3 INITIAL CONDITIONS

Table I lists the relevant aircraft state vector data measured by ARIS and the corresponding iteration rates. For systems other than ARIS, the iteration rates may, of course, differ from the

values listed in table I. In general, however, the position and velocity tracking data need to be available at a higher rate than that of the attitude and air data measurements. The reason for this will become apparent later in a discussion of the relative impact sensitivities to errors or changes in the various measured quantities.

TABLE I. RELEASE POINT DATA

Fast Loop (1/16-Second)	Slow Loop (1/2-Second)
Position (X, Y, Z)	Gimbal Angles (Pitch, Roll, Yaw)
Velocity (V_x, V_y, V_z)	Air Density
	True Airspeed
	Side-Slip Angle

The data listed in table I all have to be interpolated with respect to the release time in order to determine the aircraft state vector at release. As indicated in figure 4, "release time" is typically about 12 milliseconds after the weapon release signal reaches the weapon release rack. This 12 milliseconds is the nominal time delay necessary to fire the ejection cartridge and actuate the hook release mechanism at which time the bomb can begin to move away from the aircraft.

The foregoing procedure establishes the state vector of the aircraft at the instant of release, but what is actually needed is the state vector of the bomb at this time. Figures 5, 6, and 7 describe the corrections which ARIS makes to the aircraft state vector in order to derive the state vector of the bomb.

As indicated in figure 5, ejection velocity, expressed in aircraft coordinates, is transformed into the horizontal and vertical coordinate system. These ejection velocity components are added to the aircraft velocity components in order to calculate bomb velocity.

Similarly, the position vector of the bomb with respect to the tracking point on the aircraft is transformed from aircraft coordinates into the horizontal/vertical computational coordinate set. These lever arm corrections convert aircraft position to bomb position (see figure 6). By repeating this lever arm transformation a half second later in time, differencing the two

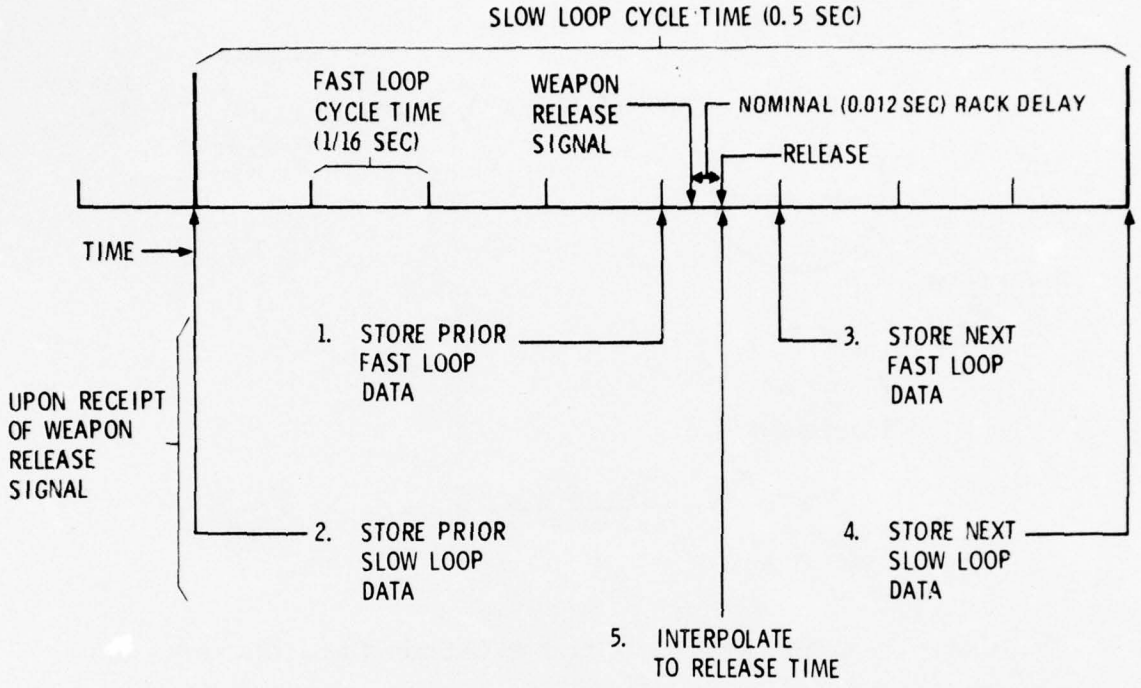

Figure 4. Interpolating to Release Point Conditions

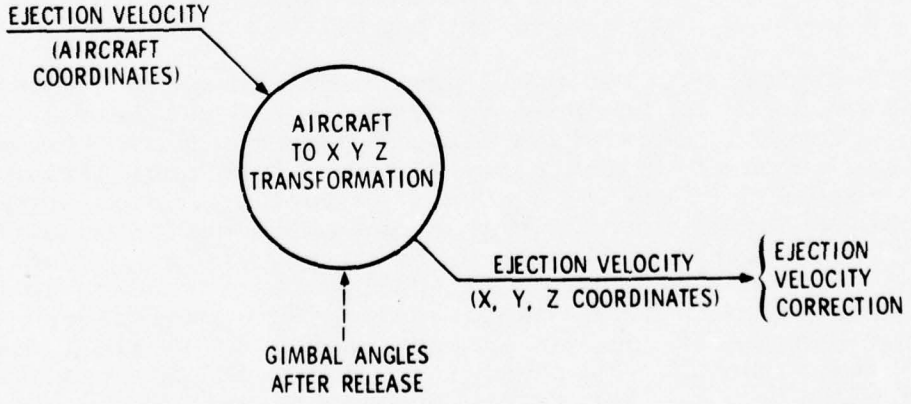

NOTE: "EJECTION VELOCITY" DOES NOT INCLUDE EFFECT OF GRAVITATIONAL ACCELERATION ACTING OVER EJECTOR FOOT EXTENSION TIME.

Figure 5. Ejection Velocity Corrections

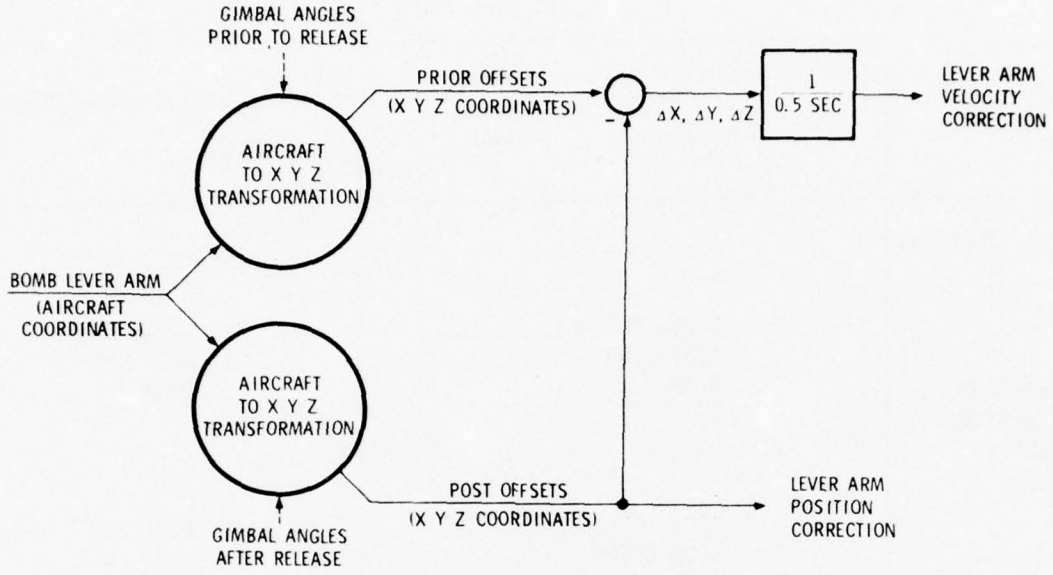

Figure 6. Bomb Lever Arm and Attitude Rate Corrections

lever arm corrections, and dividing the difference by 0.5 seconds, a measure is obtained of the effective additional velocity imparted to the bomb by attitude rates (especially rolling) at release. Thus, bomb lever arm effects give rise to a velocity correction as well as a position correction.

Figure 7 depicts another mechanism which can cause the effective initial velocity of the bomb to deviate from the release velocity of the aircraft. Separation disturbances can cause the bomb to oscillate about its pitch and yaw axes. Such oscillations create additional induced drag and give rise to lift forces normal to the bomb velocity vector, which cause it to deflect away from its predicted ballistic trajectory. Reference 2 provides an in-depth treatment of this phenomenon and points out that this is the real cause of so-called "bomb dispersion". "Bomb dispersion" is a misnomer because it implies a relationship to physical differences between bombs. Whereas, in reality, it is not a function of the bombs at all, but rather the way in which they are ejected through the disturbed airflow surrounding the aircraft. Therefore, the more accurate terminology "separation disturbances" is used in this report instead of "bomb dispersion".

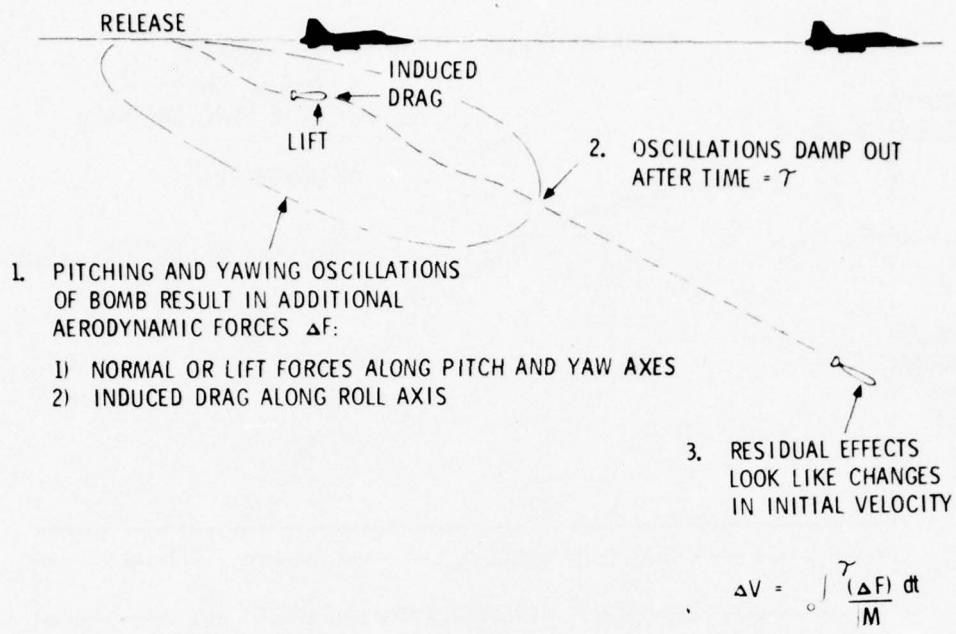

Figure 7. Separation Disturbance (Jump Velocity)

According to Reference 2, separation disturbances can be characterized by a random component superimposed on a systematic, repeatable component. The systematic, repeatable portion can be compensated for by treating it as a constant predetermined ejection-like velocity vector known as "jump velocity".

2.4 BALLISTIC TRAJECTORY SOLUTION

Having determined the initial conditions or state vector of the weapon at the start of its free fall, attention is directed to the problem of calculating the free fall trajectory of the weapon to impact. The general procedure is to solve the ballistic equations of motion by piece-by-piece integration of the differential equations which describe the motion of a point mass acted upon only by the forces of gravity and drag.

ARIS uses the so called "China Lake Trajectory Algorithm" (Reference 3) to perform this integration. It is a computationally efficient algorithm specifically designed for mechanization in airborne digital weapon delivery computers. As indicated in figure 8, it performs 10 piece-by-piece integration steps to calculate the trajectory of the bomb from release to impact. Table II lists some additional features of the algorithm, while figure 9 displays its accuracy with respect to a

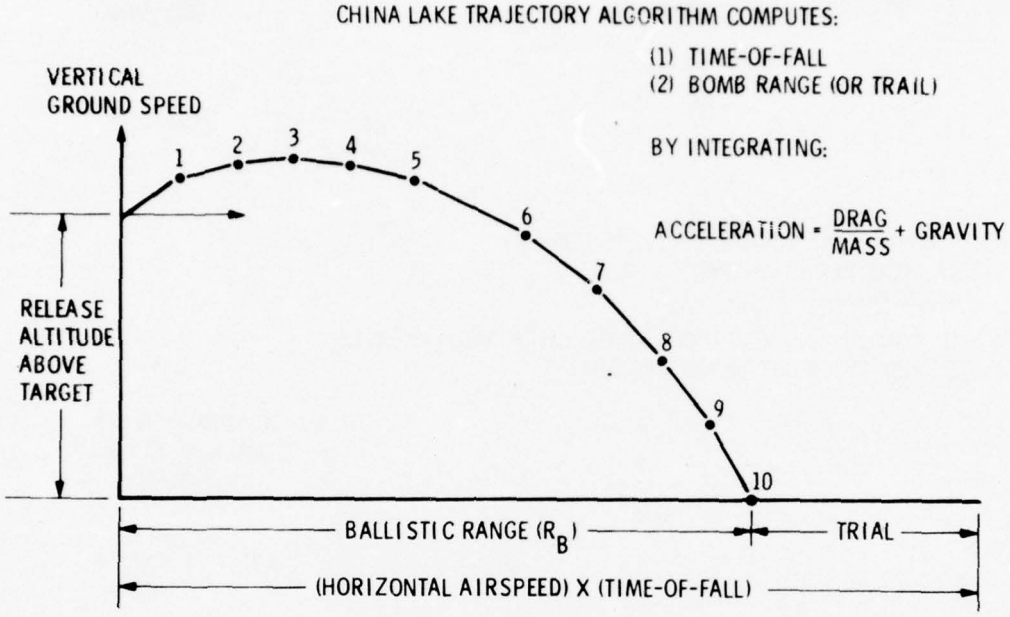

Figure 8. Vertical Plane Ballistic Trajectory Problem

TABLE II. FEATURES OF CHINA LAKE TRAJECTORY ALGORITHM

1. Models bomb drag vs mach as Mk-84 or Garve characteristics
   a. 3-Region, 2nd order polynomial curve fits
   b. Scaled and offset for different size bombs
2. Models air density variations with altitude as 2nd order polynomial
3. Models gravity as linear function of altitude
   a. ARIS modification to China Lake constant gravity model
4. Assumes flat, nonrotating earth
5. Uses 2nd order Runge-Kutta formula to integrate two-dimensional equations of motion
   a. Trajectory divided into 10 increments for piece-by-piece integration
   b. Short time increments during high acceleration
   c. Long time increments during low acceleration

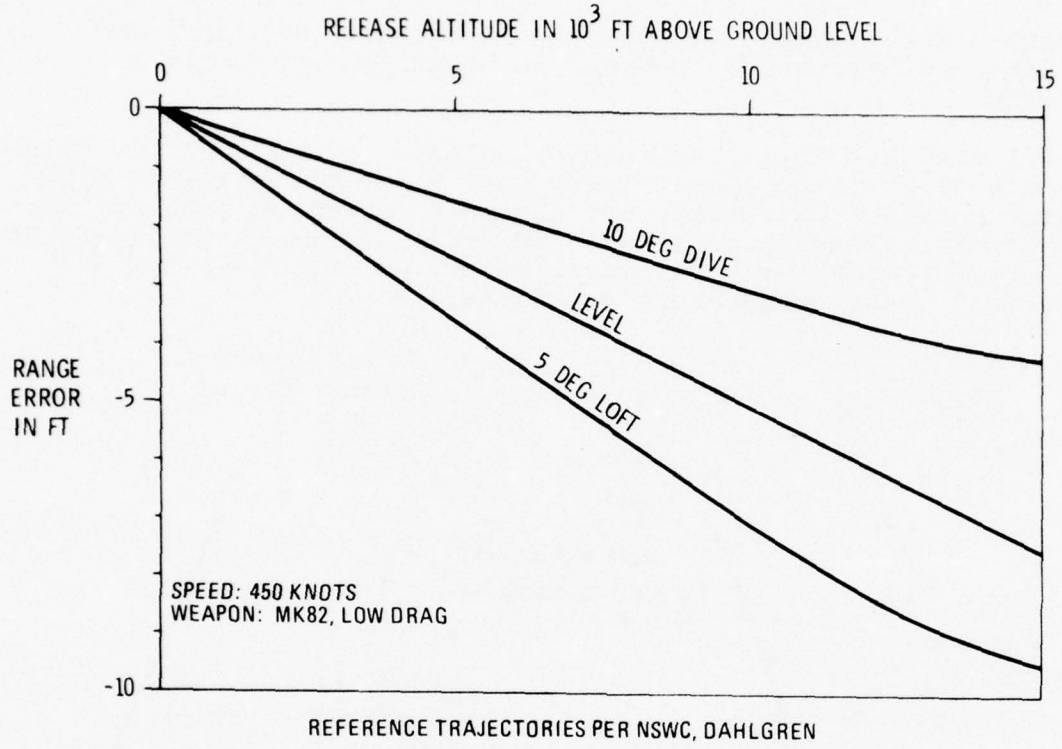

Figure 9. China Lake Ballistic Trajectory Algorithm Error

more elaborate model and integration algorithm (Reference 4). As seen therein, the errors of the algorithm for dive deliveries of low drag weapons are less than 5 feet, even for releases from as high as 15,000 feet above ground level.

One of the characteristics of the China Lake Algorithm is that it uses a flat, nonrotating earth model. This implies the need for Coriolis corrections. Because these Coriolis corrections are significant only for high bomb velocities, they need be computed only for low drag weapons. For such weapons, the analytic vacuum trajectory solution represents a sufficiently good approximation for the purpose of calculating the Coriolis corrections.

2.5 IMPACT PREDICTION SUMMARY

Figure 10 summarizes the overall impact prediction technique as mechanized in ARIS. The release point position is established by interpolating aircraft position to the time of bomb first motion and correcting for the bomb lever arm. Similarly, ground velocity of the aircraft is interpolated to bomb first motion time and

corrected for ejection velocity, attitude rate effects, and separation disturbances in order to determine bomb release velocity.

Time-of-fall and trail are then calculated by means of the China Lake trajectory algorithm. These quantities are combined with release position, velocity, and airspeed direction (determined from aircraft heading angle and side slip) as shown in figure 10 and corrected for Coriolis accelerations on the basis of analytical vacuum trajectory solutions.

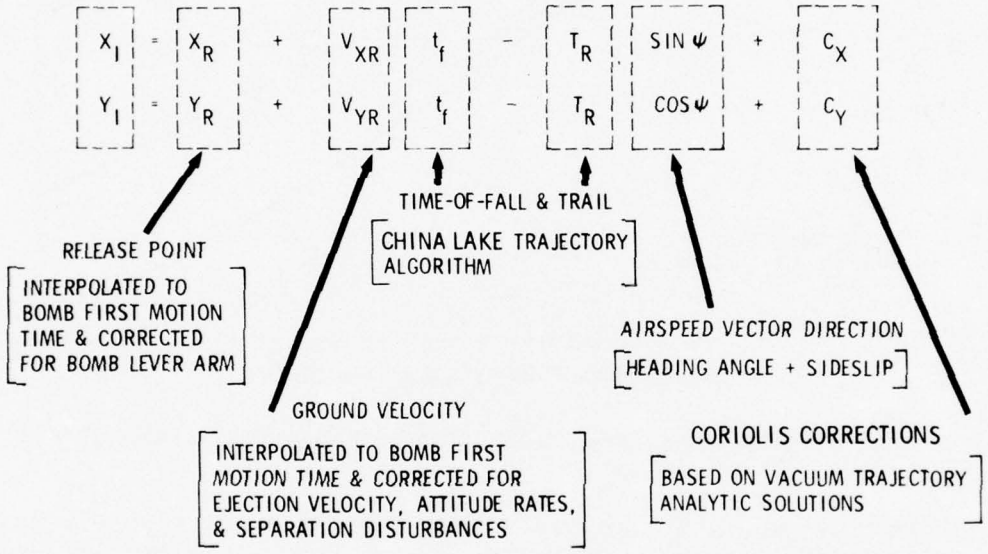

Figure 10. Impact Point Prediction Summary

SECTION III

NO-DROP WEAPON SCORING MEASUREMENTS AND ERROR SENSITIVITIES

3.1 GENERAL

3.1.1 Release Conditions

In order to conduct numerical evaluations of measurement error sensitivities, the weapon and conditions under which it is released must first be selected. Five sets of delivery conditions are considered, each of which represents typical release conditions in one of five different attack modes.

a. Dive release from 4500 feet altitude in a 35-degree dive at 550 knots. This is typical of a bomb release after visual acquisition of the target, and could represent either a dive-glide or dive-toss release (after earlier pickle in a steeper dive). Typical munitions employed in this type of attack are low-drag bombs and cluster bomblet (CBU) weapons.

b. Laydown release at 1000 feet altitude in level flight at 550 knots. The laydown release is typical of either a low-level visual bombing attack or a radar bombing attack. Normally, this mode employs a high-drag weapon.

c. Loft release at 3000 feet altitude in a 45-degree climb at 550 knots. The loft release is designed to provide the attacking aircraft with a long standoff range and, therefore, employs a low-drag bomb. This mode is useful in attacking high-threat targets (e.g., SAM sites) at known locations.

d. High-level release at 15,000 feet altitude in level flight at 450 knots. The high-level delivery mode is typical of ground-directed bombing attacks. The USMC flies this type of profile when performing blind bombing runs under TPQ-10 or TPQ-27 control. The low-drag bomb would be the typical weapon for these missions.

e. Strafing gunfire at 550 feet altitude in a 15-degree dive at 400 knots. While this may seem, on cursory examination, to be outside the scope of NDWS, it actually differs little from the problem of simulating bomb drops. Bullets are merely ballistic weapons with very high ejection velocity.

3.1.2 Weapon Type Selection

The type of weapon delivered plays an important role in the determination of error sensitivities. Herein are considered three bomb types and the 20-millimeter gun. For each of the three bomb types, the ejection velocity is assumed to be 7.5 feet per second. The muzzle velocity of the 20-mm gun is 3300 feet per second.

a. Low-drag (LD) bomb. In particular, the low-drag bomb class is represented by a Mk 82 500-pound bomb with conical fins and electric fuse.

b. Cluster bomblet (CBU) weapon. The CBU weapon is represented by a cannister which opens to disperse its bomblets five seconds after release. In this instance, the trajectory algorithm calculates the path and impact of a typical bomblet in the center of the pattern.

c. The Mk 82 Snakeye (retarded) represents the high-drag class of bombs.

3.1.3 Trajectory Solutions and Sensitivities

With the preceding definitions of delivery modes, weapons, and ejection velocities, the ballistic trajectory for each of the six cases listed in table III can be calculated. These solutions yield time-of-fall, trail, and ballistic range values as recorded in the table. The particular trajectory program used to obtain these solutions was the NSWC, Dahlgren program (Reference 4). This is the same program used to generate ballistic tables for all ballistic weapons in the U.S. Navy inventory. Table III also shows the sensitivities in ballistic range to changes in initial altitude (Z), initial horizontal velocity (V_a), initial vertical velocity (V_z), and air density (ρ). These ballistic range sensitivities are used in Section IV to compute the impact point sensitivities.

TABLE III. BALLISTIC TRAJECTORY SOLUTIONS AND SENSITIVITIES

Delivery	Weapon	t_f Time-of-Fall (Seconds)	T_R Trail (Feet)	R_B Range (Feet)	$\frac{\Delta R_B}{\Delta Z}$	$\frac{\Delta R_B}{\Delta V_a}$ (Seconds)	$\frac{\Delta R_B}{\Delta V_z}$ (Seconds)	$\frac{\Delta R_B}{\Delta \rho/\rho}$ (Feet)
Dive	Low-drag	7.089	102	5,288	0.994	6.935	6.932	-22
Dive	CBU	9.504	2,107	5,120	0.709	6.553	4.943	-682
Laydown	High-drag	10.124	5,838	3,559	0.867	1.774	3.353	-5,274
Loft	Low-drag	43.895	2,025	26,836	0.756	37.457	27.514	-2,518
High-level	Low-drag	31.256	1,254	22,500	0.716	28.450	21.180	-732
Strafe	Gun	0.661	508	2,030	3.637	0.526	1.923	-9

3.2 IMPACT SENSITIVITIES

A straightforward differentiation of the basic impact prediction equation given in figure 10 will yield the impact point sensitivities to errors in the various independent variables in the impact prediction equation. For sensitivity analyses, downrange and crossrange errors are of interest. By defining the Y and X directions to be downrange and crossrange, respectively this transformation can be written

$$D_I = D_R + V_g t_f - T_R \cos \delta + W_{cD}$$

$$C_I = C_R + V_{gC} t_f + T_R \sin \delta + W_{cC} \qquad (1)$$

where

C_I, D_I represent crossrange and downrange impact coordinates, respectively

C_R, D_R represent crossrange and downrange release coordinates, respectively

V_g, V_{gC} represent, respectively, the downrange and crossrange components of bomb ground velocity at release

t_f is the time of fall

T_R is the bomb trail

W_{cC}, W_{cD} represent, respectively, the crossrange and downrange components of Coriolis effects

δ is the drift angle or direction of the air speed vector relative to the downrange axis

Taking differentials of equation (1);

$$\Delta D_I = \Delta D_R + t_f \Delta V_g + V_g \Delta t_f - \Delta T_R \cos \delta + (T_R \sin \delta) \Delta \delta + \Delta W_{cD}$$

$$\Delta C_I = \Delta C_R + t_f \Delta V_{gC} + V_{gC} \Delta t_f + \Delta T_R \sin \delta + (T_R \cos \delta) \Delta \delta + \Delta W_{cC} \quad (2)$$

For sensitivity analysis purposes, equation (2) can be simplified by neglecting the variations, ΔW_{cD} and ΔW_{cC}, in the small Coriolis correction terms, and by assuming the nominal wind (but not the errors in computing the wind) to be zero, so that δ and V_{gC} are both zero. With these simplifications, equation (2) becomes

$$\Delta D_I = \Delta D_R + t_f \Delta V_g + V_g \Delta t_f - \Delta T_R$$

$$\Delta C_I = \Delta C_R + t_f \Delta V_{gC} + T_R \Delta \delta \quad (3)$$

Because the differential of ballistic range is somewhat more meaningful than ΔT_R, introduce the ballistic range, R_B, defined as

$$R_B = V_a t_f - T_R \quad (4)$$

where V_a is the horizontal component of airspeed at release. The differential of equation (4) is

$$\Delta R_B = t_f \Delta V_a + V_a \Delta t_f - \Delta T_R \quad (5)$$

Substituting equation (5) into equation (3) to eliminate ΔT_R, and using the zero nominal wind assumption ($V_g = V_a$), yields

$$\Delta D_I = \Delta D_R + \Delta R_B + t_f (\Delta V_g - \Delta V_a)$$

$$\Delta C_I = \Delta C_R + t_f \Delta V_{gC} + T_R \Delta\delta \qquad (6)$$

As indicated in figure 3, t_f and T_R [and hence R_B by virtue of equation (4)] are functions of release altitude (Z), release vertical velocity (V_z), true air speed (V_a), bomb drag coefficient (C_D), and air density (ρ). Any variations or errors in these quantities will cause a variation or error in R_B. The amount of variation in R_B per unit variation in one of the independent variables (Z, V_z, V_a, C_D or ρ) can be computed by means of the NSWC, Dahlgren ballistic trajectory computer program (Reference 4) by noting the change in ballistic range which results after making a small change to one of the independent variables and recomputing the ballistic range. Table III lists the corresponding sensitivities in R_B to changes in Z, V_a, V_z, and ρ for each of the six trajectory solutions. The ΔR_B sensitivity to $\Delta C_D/C_D$ is not shown separately because it is numerically equal to the sensitivity to $\Delta\rho/\rho$.

Equation (6), together with the numerical values for t_f and T_R and the ΔR_B sensitivities tabulated in table III, permit calculation of the impact error sensitivities. The subsequent paragraphs discuss each impact sensitivity in detail.

3.2.1 Sensitivity to Release Position Errors

Equation (6) shows that a 1:1 relationship exists between the horizontal release position errors (ΔD_R and ΔC_R) and the corresponding impact errors (ΔD_I and ΔC_I). The other differentials (ΔR_B, ΔV_g, ΔV_{gC}, ΔV_a, and $\Delta\delta$) are all independent of and not affected by the horizontal release position errors.

On the other hand, a vertical position error, ΔZ, at release does have an effect on ΔR_B as shown in table III. In summary, the impact sensitivities to release position errors are:

$$\Delta D_I/\Delta D_R = 1$$

$$\Delta C_I/\Delta C_R = 1$$

$$\Delta D_I/\Delta Z = \Delta R_B/\Delta Z \qquad (7)$$

Numerical values for $\Delta R_B/\Delta Z$ can be found in table III.

3.2.2 Sensitivity to Release Velocity Errors

There are actually three different types of release velocity errors, each of which propagates differently during the free fall phase. The first is ground velocity, i.e., the velocity of the bomb with respect to the ground. The second is air velocity, the velocity of the bomb with respect to the air mass. Ejection velocity, the third type, is a combination of the first two in that ejection velocity alters both the ground velocity and the air velocity by the same amount.

3.2.2.1 Ground Velocity Sensitivity. According to equation (6), the factor relating the horizontal components of ground velocity at release (ΔV_g and ΔV_{gC}) to their respective impact errors (ΔD_I and ΔC_I) is t_f, the time-of-fall. In other words, the impact error caused by a horizontal ground velocity error is equal to that error multiplied by the time-of-fall. Mathematically,

$$\Delta D_I/\Delta V_g = t_f$$

$$\Delta C_I/\Delta V_{gC} = t_f \qquad (8)$$

Table III contains numerical values for t_f.

3.2.2.2 Air Velocity Sensitivity. The two horizontal components of air velocity error are the downrange component (ΔV_a) and the crossrange component (ΔV_{aC}). From equation (6), it can be seen that a ΔV_a error affects the downrange impact error directly.

through the $-t_f\ \Delta V_a$ term, and indirectly through the ΔR_B term. Hence, the downrange error caused by a ΔV_a error is

$$\Delta D_I = \left(\frac{\Delta R_B}{\Delta V_a}\right) \Delta V_a - t_f\ \Delta V_a \tag{9}$$

The crossrange component of air velocity error (ΔV_{aC}) causes a drift angle error of amount $\Delta\delta = -\Delta V_{aC}/V_a$ which, from equation (6) causes an impact error of

$$\Delta C_I = T_R\ (-\Delta V_{aC}/V_a) \tag{10}$$

Summarizing the air velocity sensitivities indicated by equation (9) and (10) yields

$$\Delta D_I/\Delta V_a = (\Delta R_B/\Delta V_a) - t_f$$

$$\Delta C_I/\Delta V_{aC} = -T_R/V_a \tag{11}$$

Table III presents numerical values for the terms on the right-hand side of the above equations. A comparison of the numerical values of t_f and $\Delta R_B/\Delta V_a$ in this table reveals that t_f is always greater than $\Delta R_B/\Delta V_a$, which means that $\Delta D_I/\Delta V_a$ is always negative. This behavior is consistent with the definition of ΔV_a as being an increase in air speed magnitude while holding the ground velocity constant ($\Delta V_g = 0$). Hence, ΔV_a corresponds to an increased head wind and should indeed cause the computed impact point to move uprange.

3.2.2.3 <u>True Air Speed Sensitivity</u>. The horizontal air velocity (V_a) is computed from true air speed (V_t) and vertical velocity (V_z), according to the relationship

$$V_a = \sqrt{V_t^2 - V_z^2}$$

Hence, errors ΔV_t and ΔV_z in measuring true air speed and vertical velocity both cause air velocity errors, ΔV_a.

$$\Delta V_a = \frac{V_t}{V_a} \Delta V_t - \frac{V_z}{V_a} \Delta V_z$$

$$= \frac{\Delta V_t}{\cos \gamma} - \frac{\Delta V_z}{\text{ctn } \gamma} \qquad (12)$$

When the ΔV_t part of equation (12) is substituted into equation (11), the impact sensitivity to ΔV_t is found to be

$$\frac{\Delta D_I}{\Delta V_t} = \frac{1}{\cos \gamma} \left[\left(\frac{\Delta R_B}{\Delta V_a} \right) - t_f \right] \qquad (13)$$

Table III contains the numerical values of the quantities necessary to evaluate equation (13).

3.2.2.4 Vertical Velocity Sensitivity. Vertical velocity is both a ground velocity and an air velocity, because the impact prediction equation, equation (1), contains no provision for updrafts or downdrafts. The presumption is that the air mass has no vertical component of motion. For this reason, vertical velocity is treated separately instead of trying to classify it under "ground velocity" or under "air velocity."

The impact sensitivity to vertical velocity error (ΔV_z) at release comes about for two reasons. First, ΔV_a is sensitive to ΔV_z as indicated in equation (12). Secondly, ΔR_B is also sensitive to ΔV_z, both directly, as indicated in table III, and indirectly through ΔV_a and equation (12). Combining all of these ΔV_z effects into equation (6) results in

$$\Delta D_I = \left(\frac{\Delta R_B}{\Delta V_z} \right) \Delta V_z + \left(\frac{\Delta R_B}{\Delta V_a} \right) \left(- \frac{\Delta V_z}{\text{ctn } \gamma} \right) - t_f \left(- \frac{\Delta V_z}{\text{ctn } \gamma} \right)$$

$$= \left[\frac{\Delta R_B}{\Delta V_z} + \left(t_f - \frac{\Delta R_B}{\Delta V_a} \right) \tan \gamma \right] \Delta V_z \qquad (14)$$

Summarizing the above, the vertical velocity sensitivity becomes

$$\frac{\Delta D_I}{\Delta V_z} = \frac{\Delta R_B}{\Delta V_z} + \left(t_f - \frac{\Delta R_B}{\Delta V_a} \right) \tan \gamma \qquad (15)$$

The terms on the right-hand side of the above equation can be evaluated numerically from table III.

3.2.2.5 Ejection and/or Jump Velocity Sensitivity. The vertical component of ejection or jump velocity error (ΔV_{Ez}) has the same effect as the foregoing vertical velocity error. That is

$$\frac{\Delta D_I}{\Delta V_{Ez}} = \frac{\Delta D_I}{\Delta V_z} \qquad (16)$$

where $\Delta D_I / \Delta V_z$ is given by equation (15). Ejection or jump velocity can also have horizontal components, due either to a nonvertical orientation of the ejection or separation disturbance force relative to the aircraft or to a non-level attitude of the aircraft at release. These horizontal components create errors in both ground velocity and air velocity of equal amounts. The impact sensitivity, therefore, is the sum of the sensitivities to ground and air velocities. Accordingly, using equations (4), (8), and (11):

$$\frac{\Delta D_I}{\Delta V_{ED}} = \frac{\Delta D_I}{\Delta V_g} + \frac{\Delta D_I}{\Delta V_a}$$

$$= t_f + \frac{\Delta R_B}{\Delta V_a} - t_f = \frac{\Delta R_B}{\Delta V_a} \qquad (17)$$

$$\frac{\Delta C_I}{\Delta V_{Ec}} = \frac{\Delta C_I}{\Delta V_{gc}} + \frac{\Delta C_I}{\Delta V_{ac}}$$

$$= t_f - \frac{T_R}{V_a} = \frac{R_B}{V_a} \qquad (18)$$

Equations (16), (17), and (18) express the impact sensitivities to errors in ejection velocity where the ejection velocity is expressed in downrange, crossrange, and vertical coordinates. However, ejection velocity is typically specified in aircraft coordinates and must be transformed into horizontal and vertical components. For example, in wings-level flight (zero roll angle), a yaw axis ejection velocity ($V_{E\psi}$) has downrange and vertical components, respectively, of amount

$$V_{ED} = -V_{E\psi} \sin \theta$$

$$V_{Ez} = V_{E\psi} \cos \theta \tag{19}$$

Hence, the downrange impact error, ΔD_I, caused by an error $\Delta V_{E\psi}$ in the yaw axis component of the ejection or jump velocity is

$$\Delta D_I = \frac{\Delta D_I}{\Delta V_{ED}} (-\Delta V_{E\psi} \sin \theta) + \frac{\Delta D_I}{\Delta V_{Ez}} (\Delta V_{E\psi} \cos \theta)$$

$$= \left[-\frac{\Delta R_B}{\Delta V_a} \sin \theta + \frac{\Delta D_I}{\Delta V_z} \cos \theta \right] \Delta V_{E\psi} \tag{20}$$

Similarly, a roll axis ejection or jump velocity $V_{E\phi}$ has downrange and vertical components, respectively, of amount

$$V_{ED} = V_{E\phi} \cos \theta$$

$$V_{Ez} = V_{E\phi} \sin \theta \tag{21}$$

The downrange impact error due to an error $\Delta V_{E\phi}$ in the roll axis component of ejection or jump velocity is

$$\Delta D_I = \frac{\Delta D_I}{\Delta V_{ED}} (\Delta V_{E\phi} \cos \theta) + \frac{\Delta D_I}{\Delta V_{Ez}} (\Delta V_{E\phi} \sin \theta)$$

$$= \left[\frac{\Delta R_B}{\Delta V_a} \cos \theta + \frac{\Delta D_I}{\Delta V_z} \sin \theta \right] \Delta V_{E\phi} \tag{22}$$

For wings-level flight, the pitch axis of the aircraft corresponds to the crossrange axis, and equation (18) applies for errors in the pitch axis component of ejection or jump velocity ($\Delta V_{E\theta} = \Delta V_{EC}$).

In summary, the impact sensitivities to ejection and jump velocity errors for wings-level flight, are as shown below:

$$\frac{\Delta D_I}{\Delta V_{E\psi}} = -\left(\frac{\Delta R_B}{\Delta V_a}\right)\sin\theta + \left(\frac{\Delta D_I}{\Delta V_z}\right)\cos\theta$$

$$\frac{\Delta D_I}{\Delta V_{E\phi}} = \left(\frac{\Delta R_B}{\Delta V_a}\right)\cos\theta + \left(\frac{\Delta D_I}{\Delta V_z}\right)\sin\theta$$

$$\frac{\Delta C_I}{\Delta V_{E\theta}} = \frac{R_B}{V_a} \qquad (23)$$

Table III and equation (15) supply the necessary numerical values and expressions needed to evaluate the above equations, once that θ is known. For the sensitivity analysis evaluations herein, the approximation $\theta = \gamma$ is made. In other words, the pitch angle (θ) is approximated by the flight path angle (γ).

3.2.3 Sensitivity to Aircraft Attitude Errors

Aircraft attitude errors cause an error in calculating the direction of the ejection velocity. For example, if the ejection velocity (V_E) is directed downward along the negative yaw axis of the aircraft ($V_E = -V_{E\psi}$), then pitch and roll errors ($\Delta\theta$, $\Delta\phi$, respectively) will cause ejection velocity component errors of amounts

$$\Delta V_{E\phi} = V_E \Delta\theta$$

$$\Delta V_{E\theta} = -V_E \Delta\phi \qquad (24)$$

The resulting downrange and crossrange impact errors are

$$\Delta D_I = \left(\frac{\Delta D_I}{\Delta V_{E\phi}}\right) V_E \Delta\theta$$

$$\Delta C_I = \left(\frac{\Delta C_I}{\Delta V_{E\theta}}\right) (- V_E \Delta\phi) \qquad (25)$$

An error $\Delta\psi$ in measuring aircraft heading causes an equal and opposite error ($\Delta\delta = -\Delta\psi$) in determining drift angle. From equation (6):

$$\Delta C_I = T_R \Delta\delta = - T_R \Delta\psi \qquad (26)$$

Summarizing equations (25) and (26) with the aid of equation (23) yields

$$\frac{\Delta D_I}{\Delta\theta} = V_E\left[\left(\frac{\Delta R_B}{\Delta V_a}\right) \cos\theta + \left(\frac{\Delta D_I}{\Delta V_z}\right) \sin\theta\right]$$

$$\frac{\Delta C_I}{\Delta\phi} = -V_E \frac{R_B}{V_a}$$

$$\frac{\Delta C_I}{\Delta\psi} = -T_R \qquad (27)$$

Given values for V_E and θ, the above expressions can be evaluated readily using table III and equation (15). For the purpose of this analysis, V_E was set equal to 7.5 fps, and θ was set equal to the flight path angle at release.

Theoretically, attitude measurement errors introduce an additional impact error through incorrect computation of the bomb lever arm components. In most cases, however, these lever arms are all less than 20 feet, and a 20-milliradian error at the end of a 20-foot lever arm is only 0.4 feet. This is a negligible contribution to the impact error and can safely be omitted.

3.2.4 Sensitivity to Aircraft Attitude Rate Errors

Although the position errors resulting from a rotation of the bomb lever arm through the attitude errors are negligible, the velocity errors resulting from attitude rate errors in this lever arm compensation process, are not. Assuming that the bomb lever arm has a pitch axis ($L_{B\theta}$) component but negligible roll and yaw axis components ($L_{B\phi} = L_{B\psi} = 0$) the equivalent ejection velocity error can be calculated as

$$\Delta V_{E\psi} = -L_B \ \Delta\dot{\phi}$$

$$\Delta V_{E\phi} = -L_{B\theta} \ \Delta\dot{\psi} \qquad (28)$$

Using equation (28) to expand ΔD_I in equation (6) results in

$$\Delta D_I = \frac{\Delta D_I}{\Delta V_{E\psi}} (-L_{B\theta} \ \Delta\dot{\phi}) + \frac{\Delta D_I}{\Delta V_{E\phi}} (-L_{B\theta} \ \Delta\dot{\psi}) \qquad (29)$$

With the aid of equation (23), equation (29) can be used to summarize the attitude rate sensitivities as follows:

$$\frac{\Delta D_I}{\Delta\dot{\phi}} = L_{B\theta} \left[\left(\frac{\Delta R_B}{\Delta V_a} \right) \sin\theta - \left(\frac{\Delta D_I}{\Delta V_z} \right) \cos\theta \right]$$

$$\frac{\Delta D_I}{\Delta\dot{\psi}} = -L_{B\theta} \left[\left(\frac{\Delta R_B}{\Delta V_a} \right) \cos\theta + \left(\frac{\Delta D_I}{\Delta V_z} \right) \sin\theta \right] \qquad (30)$$

Using a value for $L_{B\theta}$ equal to 10 feet and setting θ equal to γ, the attitude rate sensitivities can be calculated from the above equations, table III, and equation (15).

3.2.5 Sensitivity to Air Density Errors

Air density (ρ) is related to the static air temperature (T_S) and pressure (P_S) according to the perfect gas law

$$\rho = \frac{P_S}{R_C T_S} \qquad (31)$$

where R_C is the gas constant for atmospheric air.

As a consequence, an air temperature error (ΔT_S) causes a density error of

$$\Delta\rho = -\rho \frac{\Delta T_S}{T_S} \tag{32}$$

Likewise, an air pressure measurement error (ΔP_S) causes a density error of

$$\Delta\rho = \rho \frac{\Delta P_S}{P_S} \tag{33}$$

From equation (6),

$$\Delta D_I = \left(\frac{\Delta\rho}{\rho}\right)\left[\frac{\Delta R_B}{(\Delta\rho/\rho)}\right] \tag{34}$$

Table III lists numerical values of $\Delta R_B/\Delta\rho/\rho$ for the various release conditions of interest herein.

Summarizing the air density measurement errors from equations (32) and (34) and from equations (33) and (34), yields

$$\frac{\Delta D_I}{(\Delta T_S/T_S)} = -\frac{\Delta R_B}{\Delta\rho/\rho}$$

$$\frac{\Delta D_I}{(\Delta P_S/P_S)} = \frac{\Delta R_B}{\Delta\rho/\rho} \tag{35}$$

Table III provides the necessary numerical values for the quantity on the right-hand side of equation (35).

3.3 SUMMARY AND CONCLUSIONS

Table IV summarizes the numerical values of the impact sensitivities for the six typical trajectories listed in table III. The numerical values designate the ground plane miss in feet per unit change in the measurement quantity. For example, the figure 43.9 in the horizontal velocity column for the loft delivery means that each foot per second change in horizontal velocity at the release point causes a 43.9-foot change in the ground plane impact point.

If it is desired to make the NDWS as accurate as the weapon dispersion, then it is perhaps more appropriate to express the impact sensitivities in terms of mils instead of ground plane miss distances, because weapon dispersion is typically expressed in mils. For this purpose

$$\Delta D_M = \frac{\Delta D_I \times 10^3}{\sqrt{R_B^2 + Z^2}\sqrt{1 + (\Delta R_B/\Delta Z)^2}}$$

$$\Delta C_M = \frac{\Delta C_I \times 10^3}{\sqrt{R_B^2 + Z^2}} \qquad (36)$$

where ΔD_M = downrange miss in mils

ΔC_M = crossrange miss in mils

Equation (36) computes mils as the angle in milliradians obtained by dividing the minimum distance between the trajectory and the target by the slant range at release point. The quantity $\sqrt{R_B^2 + Z^2}$ is the slant range at release. The factor $[1 + (\Delta R_B/\Delta Z)^2]^{-1/2}$ is the sine of the impact angle and projects a ground plane downrange miss into a plane normal to the impact trajectory. The factor 10^3 converts radians to milliradians.

Using the above definition of mils and assuming the scoring accuracy criteria for weapon dispersion shown in table V, it becomes possible to determine how large an error can be tolerated in each of the measurement quantities shown in table IV before that error alone causes the scoring error to equal the weapon dispersion. Table V presents these figures for the six typical delivery modes listed in tables III and IV.

Because each of the measurement tolerance values listed in table V would, by itself, cause an error equal to the assumed weapon dispersion, the final specification values for each measurement error must be less than the values listed in the table. However, table V presents a good comparison of the relative importance of each of the various measurements in each of the six delivery modes. The lowest value in each of the Quantities Measured at Release columns of table V (excluding the strafe mode which is considered separately) is encircled to

TABLE IV. IMPACT SENSITIVITIES

Delivery	Weapon	Quantities Measured at Release									
		Position (Ft)		Velocity (F_{PS})		Attitude (Degrees)			Roll Rate (Deg/Sec)	Air Data	
		Horiz.	Vert.	Horiz.	Vert.	Pitch	Roll	Heading		TAS (F_{PS})	P-T (%)
Dive	Low-drag	1	0.99	7.1	6.8	0.2	0.9	1.8	1.7	0.2	0.2
Dive	CBU	1	0.71	9.5	2.9	0.5	0.9	36.8	1.1	3.6	6.8
Laydown	High-drag	1	0.87	10.1	3.4	0.2	0.1	101.9	0.6	8.4	52.7
Loft	Low-drag	1	0.76	43.9	34.0	6.6	3.8	35.3	0.4	9.1	25.2
High-level	Low-drag	1	0.72	31.3	21.2	3.7	3.9	21.9	3.7	2.8	7.3
Strafe	Gun	1	3.64	0.66	1.9	113.0	-	29.5	0.3	0.1	0.1

NOTE: Numerical values indicate ground plane impact sensitivity in feet per unit change in measured quantity.

TABLE V. REQUIRED MEASUREMENT ACCURACIES

Scoring accuracy criteria (mils):

High-drag bombs	9
Cluster bomblet (CBU)	6
Low-drag bombs	3
Guns	1.5

NOTES:

1. Values represent minimum measurement accuracy needed to meet the stated criteria.
2. Circled quantities are worst-case values, excluding strafe mode

Delivery	Weapon	Quantities Measured at Release									
		Position (Ft)		Velocity (F_{PS})		Attitude (Degrees)			Roll Rate (Deg/Sec)	Air Data	
		Horiz.	Vert.	Horiz.	Vert.	Pitch	Roll	Heading		TAS (F_{PS})	P-T (%)
Dive	Low-drag	(21)	(30)	2.9	4.3	*	23	12	18	155	*
Dive	CBU	41	71	4.3	17.4	*	46	1.1	47	13.9	7.4
Laydown	High-drag	33	51	3.3	13.1	*	*	(0.33)	75	(5.3)	(0.8)
Loft	Low-drag	81	134	(1.8)	(3.0)	(15)	21	2.3	235	11.1	4.0
High-level	Low-drag	81	139	2.6	4.7	22	(21)	3.7	(6)	35	13.6
Strafe	Gun	3.2	3.3	4.8	6.3	0.11	*	0.11	147	85	

*Designates greater than 90 degrees or 100 percent.

indicate the maximum acceptable measurement tolerances for scoring bomb drops in all of the listed bombing modes. Scrutiny of the circled values leads to the following conclusions:

a. A "no-drop" bomb scoring system can solve dive, laydown, loft, and high-level bombing problems to accuracies commensurate with bomb dispersion provided that the following measurement accuracies are attained:

Horizontal position:	20 feet
Vertical position:	30 feet
Horizontal velocity:	2 feet per second
Vertical velocity:	3 feet per second
Heading:	0.3 degrees
Roll rate:	6 degrees per second
True airspeed:	5 feet per second
Air pressure and temperature	1 percent

b. A strafe scoring system would require position measurement accuracy of 3 feet; pitch and heading measurement accuracy of 0.1 degrees.

SECTION IV

NO-DROP WEAPON SCORING IMPLEMENTATION

4.1 GENERAL

The preceding section established which quantities the NDWS system must measure and the accuracy required of these measurements. Some representative numerical examples to establish upper limits on the measurement tolerances were also presented. This section directs attention to the problem of implementation or mechanization of a NDWS system which can achieve these measurement accuracies.

One question which arises is whether the sensors should be ground-based or airborne. From an aircraft operations viewpoint, it is desirable to avoid airborne sensors. However, from a realistic training viewpoint, ground-based sensors should be avoided. In all probability, the final configuration of NDWS will represent a compromise between these two conflicting viewpoints.

Table VI lists the various quantities which must be measured. It should be noted that pitch and roll are omitted because it was shown (in table V) that the allowable tolerance on these quantities for bomb scoring is sufficiently large to render measurement unnecessary. This would not, of course, hold true for strafe scoring. Table VI suggests several different methods for measuring the various quantities needed for no-drop bomb scoring, and categorizes these methods as totally airborne, totally ground-based, or a combination of the two. It can be seen from the table that no entirely ground-based system can supply all of the required measurements. Furthermore, no totally airborne system can perform the NDWS task because airborne inertial sensors cannot provide the required position accuracy (better than 20 feet). The inescapable conclusion is that the NDWS system must be an admixture of these techniques.

4.2 COMBINING POSITION AND VELOCITY DATA

Since it becomes necessary to combine ground-based and airborne sensor data, this is best accomplished in a manner which utilizes the most salient features of each sensor type. For example, the primary advantage of radar or DME is long-term positional accuracy, while the best feature of airborne inertial sensing is its ability to follow changes in aircraft position, velocity, and acceleration, essentially without dynamic lag. A general method for combining position tracking (e.g., radar) and inertially-sensed data and which does incorporate the best features of each, is formulated below.

TABLE VI. MEASUREMENT TECHNIQUES

Quantity Measured	Location of Sensors		
	Ground	Ground and Airborne	Airborne
Position	Radar	DME Beacon radar	Inertial
Velocity	Doppler radar	Doppler DME	Inertial
Heading	–	–	Heading reference Inertial
Roll rate	–	–	Roll rate gyro Inertial
Airspeed, Pressure, Temperature	Ground level Wind, Pressure, Temperature	–	Air data probe and computer

Although radar is used in this exposition as an example, the same technique may be applied to any other type of position tracker such as a laser tracker, cinetheodolite network, or DME multilateration system. The following is a step-by-step description of the process of combining radar and inertial data. Figure 11 illustrates this process graphically.

a. Record or telemeter inertial position and velocity (approximately 10 times per second).

b. Record radar position (approximately 100 times per second).

c. Interpolate radar position data to times of inertial data recording.

d. Difference inertial and radar position data to obtain a measure of inertial position error vs time.

e. Smooth and differentiate inertial position error vs time to obtain inertial velocity error vs time.

f. Interpolate raw inertial position and velocity data to release time.

g. Subtract inertial errors at release time from raw inertial release data to obtain corrected release position and velocity.

The basic technique is to compare inertially-derived position with radar-measured position and to plot this difference against time. The result is a band of data points as shown in figure 11c. Each point represents the difference between inertial position and radar position at that point in time. The width of the band of data points is due to high-frequency radar noise because inertially-derived position data are the result of a double integration process, and its error changes slowly with time. This high-frequency noise can be filtered or smoothed by fitting a least-squares, "best fit", low-order (e.g., second order) polynomial curve through the data points. To the extent that this best fit curve has smoothed out the radar noise, it now represents the slowly varying error in inertial position as a function of time. Furthermore, since its slope is the time rate of change of inertial position error, it is a measure of inertial velocity error.

Because inertial velocity error in an inertial system changes slowly with time, the smoothing time available for determining the slope of the best fit curve in figure 11c is at least many seconds and perhaps as long as several minutes, provided that radar tracking data are available for that period of time. This means that the inertial velocity error at release can be obtained with great accuracy and used to correct the release velocity as recorded by the raw inertial data at release. Similarly, the value of the best fit inertial position error curve at the release time provides the amount of correction to be applied to the raw inertial position data at release.

This discussion of combining inertial and radar data has considered only a single coordinate component of position and velocity. However, the process described above can be applied individually to each of the three coordinate components of position and velocity.

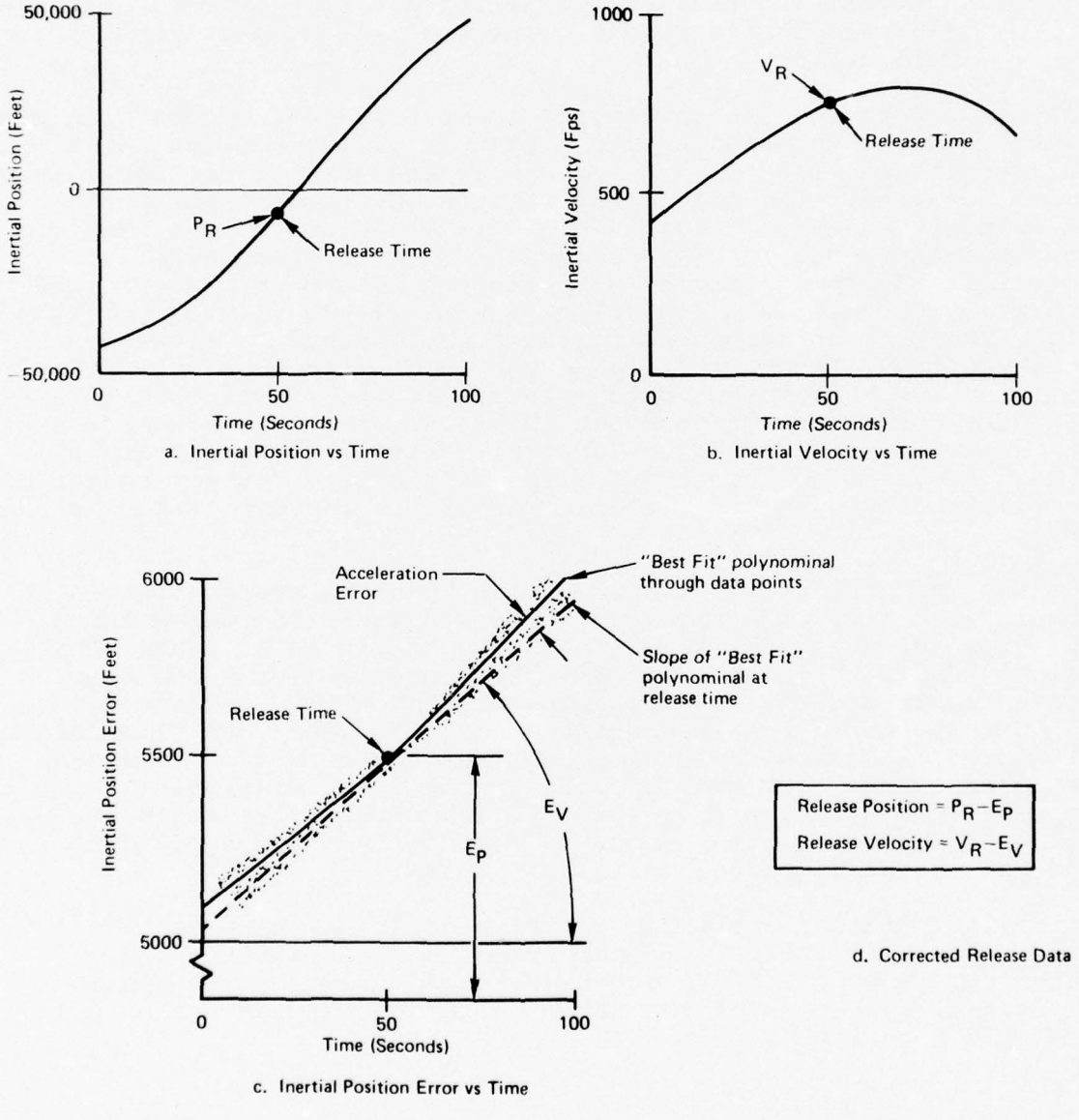

Figure 11. Release State Vector from Combined Radar-Inertial Data

4.3 ERROR TRADE-OFFS

This method outlined in paragraph 4.2 provides dynamically correct measurements of:

a. Release position which is as accurate as the accuracy of the smoothed radar position, and

b. Release velocity which is approximately as accurate as the ratio of the accuracy of the smoothed radar position to the smoothing time.

The available smoothing time is a function of the acceleration measurement error in the inertial system. If the smoothing time is restricted (somewhat arbitrarily, but logically) to that time within which the position error caused by acceleration error is less than or equal to the standard deviation of the position tracking data, the smoothing time can be estimated as follows:

$$\sigma_p = \frac{1}{2}\,\sigma_A\,t_s^2$$

$$t_s = \sqrt{\frac{2\sigma_p}{\sigma_A}}$$

where

σ_A = acceleration error (1σ)

σ_p = position tracking error (1σ)

t_s = smoothing time

The resulting velocity error (1σ) would be

$$\sigma_v = \frac{\sigma_p}{t_s} = \sqrt{\frac{\sigma_A\,\sigma_p}{2}} \qquad (39)$$

Figure 12 is a plot of equation (39). It displays the velocity accuracy (σ_v) attainable as a function of the position tracking accuracy (σ_p) and the acceleration measurement accuracy (σ_A). On this chart, various levels of position accuracy (σ_p) with various methods of tracking can be identified. For example, a laser tracker can achieve position accuracy of 1 to 2 feet; a

cinetheodolite network, 2 to 5 feet; a DME multilateration system, 5 to 10 feet; and a radar, 10 to 20 feet as indicated in figure 12.

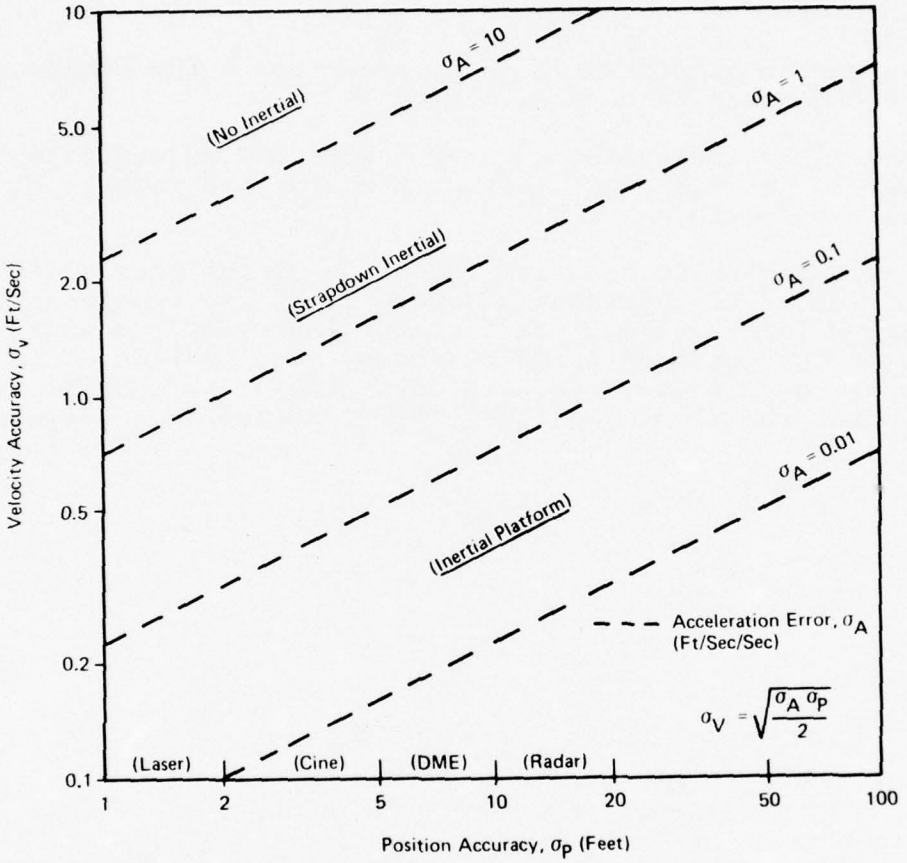

Figure 12. Position/Acceleration Accuracy Trade-Off

Similarly, various levels of inertial sensing accuracy can be identified using the acceleration error parameter (shown by broken lines in figure 12). For example, an inertial platform can measure acceleration to an accuracy of 10^{-4}g or 0.03 ft/sec^2, while a strapdown inertial system can measure acceleration to an accuracy of 1 ft/sec^2. With no inertial sensing, the acceleration error is equal to aircraft acceleration (which may be in the neighborhood of 1g). The acceleration error accuracy for each of these measurement techniques has been located on the graph (figure 12) for illustrative purposes.

Figure 12 now shows the quality of the velocity measurement achievable with various combinations of inertial and position sensors. For example, it indicates that a DME in combination with an inertial platform can determine velocity to an accuracy of about 0.3 feet per second. The ARIS is this type of system and does, in fact, achieve this degree of velocity accuracy as can be seen by examination of the ARIS flight test results in Section V. Alternatively, according to figure 12, radar tracking data combined with strapdown inertial data could achieve a velocity accuracy of approximately 3 feet per second. The measurement accuracy tolerances shown in table V indicate this approaches satisfaction of the NDWS requirement. In fact, if attention is restricted to the DME and radar systems as the only viable all-weather position sensors, it can be seen that the strapdown inertial sensor, at best, achieves only marginally acceptable velocity accuracy with either system. On the other hand, the inertial platform satisfies the NDWS velocity measurement requirement by a comfortable margin when combined with either DME or radar.

4.4 CONCLUSIONS

This analysis of no-drop weapon scoring implementation results in the following conclusions:

a. Proper implementation of the NDWS will necessarily contain both ground-based and airborne sensing elements.

b. Strapdown inertial data combined with either DME or radar position tracking data can, at best, achieve only marginally acceptable velocity data for NDWS.

c. Inertial platform data combined with either DME or radar position tracking data, can satisfy the NDWS accuracy requirement by a comfortable margin.

SECTION V

ARIS

5.1 GENERAL

Because ARIS represents a relatively new approach to no-drop weapon scoring, this section is devoted to a brief description of ARIS and its flight test results. The nomenclature "ARIS" is a Litton acronym for Airborne Range Instrumentation System. This system was designed as a bomb scoring system in support of the DDR & E program known as RABVAL, the object of which was to evaluate the radar bombing capabilities of modern weapons systems (F111F and A6E) under realistic operational conditions. As such, the ARIS was required to score simulated bombing attacks accurately and rapidly. These simulated attacks were made by F111F and A6E aircraft against unfamiliar targets while using realistic tactics. The following are the more specific requirements which formed the basis for the design of ARIS. The 20-foot CEP accuracy requirement was intended to provide a scoring system which was much more accurate than the weapon delivery system being scored.

a. High accuracy: 20 feet CEP

b. Mobile target area equipment: man-portable

c. Unrestricted delivery modes: Dive, level, loft, pull-up and breakaway at all speeds, all altitudes, and using all bomb types

d. No operational constraints: Any azimuth approach, all-weather operation, no aircraft modifications, immediate data availability

The requirement for highly mobile target area equipment arose from the test requirement to score simulated bombing against realistic, off-range targets which were totally unfamiliar to the aircrews. Typical targets were dams, bridges, storage silos, and buildings. The target instrumentation could be set up daily on a temporary basis and changed frequently. This provided the aircrews with a new set of targets which they had not previously "attacked", and served to minimize complaints from the local populace.

The requirement to score any possible delivery mode stems from the general need to permit the "attacking" aircraft to employ realistic tactics. One such tactic is very low-level penetration and attack designed to avoid enemy radar. A radar bomb scoring (RBS) site experiences great difficulty in scoring such a tactic because, if it is performed successfully, the RBS cannot track the aircraft to score it. ARIS, however, has successfully scored simulated runs at altitudes above ground level (AGL) as low as 200 feet and as high as 24,000 feet.

Perhaps the most restrictive of the requirements prohibiting operational constraints is the disallowing of aircraft modifications. This virtually limits the airborne equipment to a pod which must mount on a standard weapon release rack and use only the electrical power and control signals (e.g., weapon release signal) already available at that station.

In the subsequent paragraphs, the system known as ARIS which Litton designed and built to satisfy these stringent requirements is described.

5.2 DESCRIPTION OF ARIS

5.2.1 Major Elements

Figure 13 illustrates the major elements of ARIS. Target area instrumentation consists of an array of transponders, typically four in number, arranged around the target. One transponder, designated the central transponder, is on or close to the target. The others are located approximately a mile distant along radii separated from each other azimuthally by about 120 degrees. The transponders are man-portable and easily moved from one target site to another by automobile, truck, jeep, or helicopter. The transponders provide a series of ground reference points for the airborne pod. As such, their positions with respect to the target must be presurveyed precisely to an accuracy of about one foot. However, it is not necessary to know the exact latitude and longitude coordinates of the target.

The airborne portion of ARIS fits into a pod which attaches to a standard, unmodified weapon pylon station on the attack aircraft. Ground handling and loading of the pod is accomplished by the ground crew in essentially the same manner as handling and loading of a bomb.

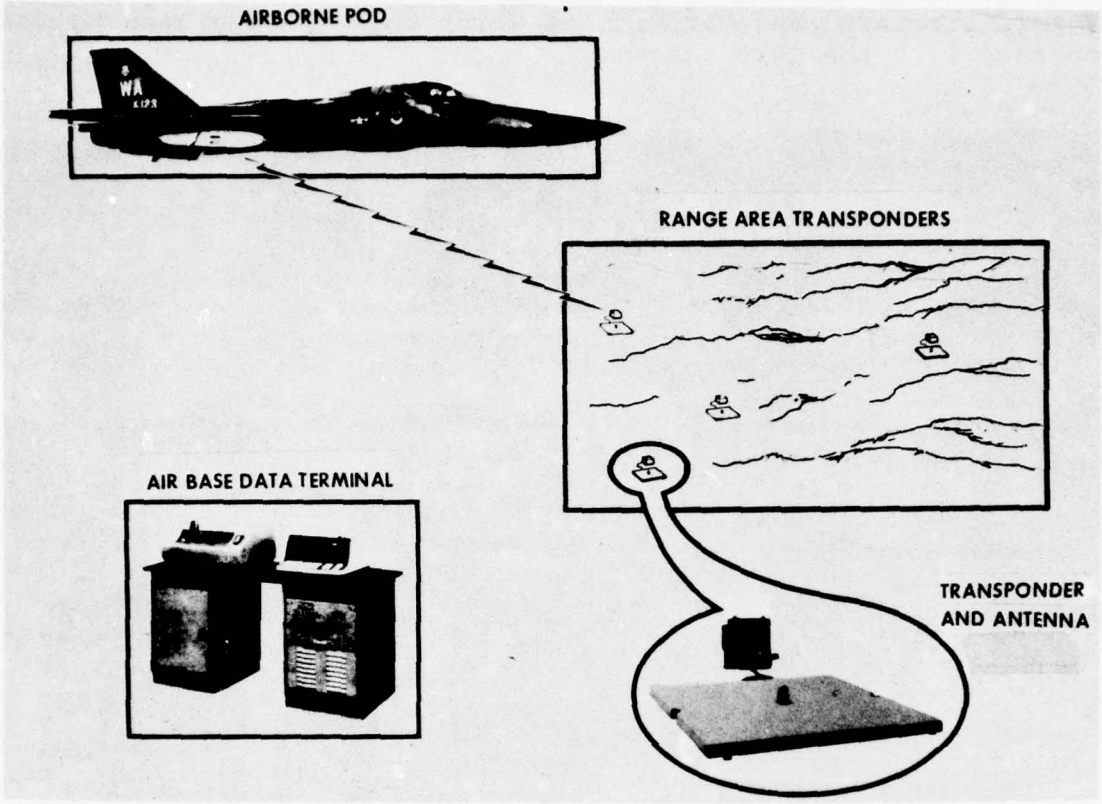

Figure 13. Major Elements of ARIS

A data terminal is located at the air base from which the attack aircraft operates. This data terminal reads the data from a magnetic tape which was recorded in the pod during the bomb scoring mission. The data terminal then formats and prints out the data to provide a permanent hard copy record of each mission.

Figure 14 shows the relative locations of the various units contained in the airborne pod. The ARIS pod is 22 inches in diameter, 16 feet in length, and weighs 800 pounds. It attaches to a standard aircraft weapon pylon station with 30-inch spacing between the two mounting lugs.

The size of the ARIS pod used on the RABVAL program was governed by the size of the subsystems which were readily available in 1973. Using current state-of-the-art subsystems, pod size can be reduced to the size of a MK 82 bomb. In fact, some types of aircraft (A6E and A7D, for example) need not carry a pod at all, provided that inertial and air data information is already

accessible in digital form. This would hold especially true of future aircraft, the avionics of which could be designed to operate with the NDWS ranges.

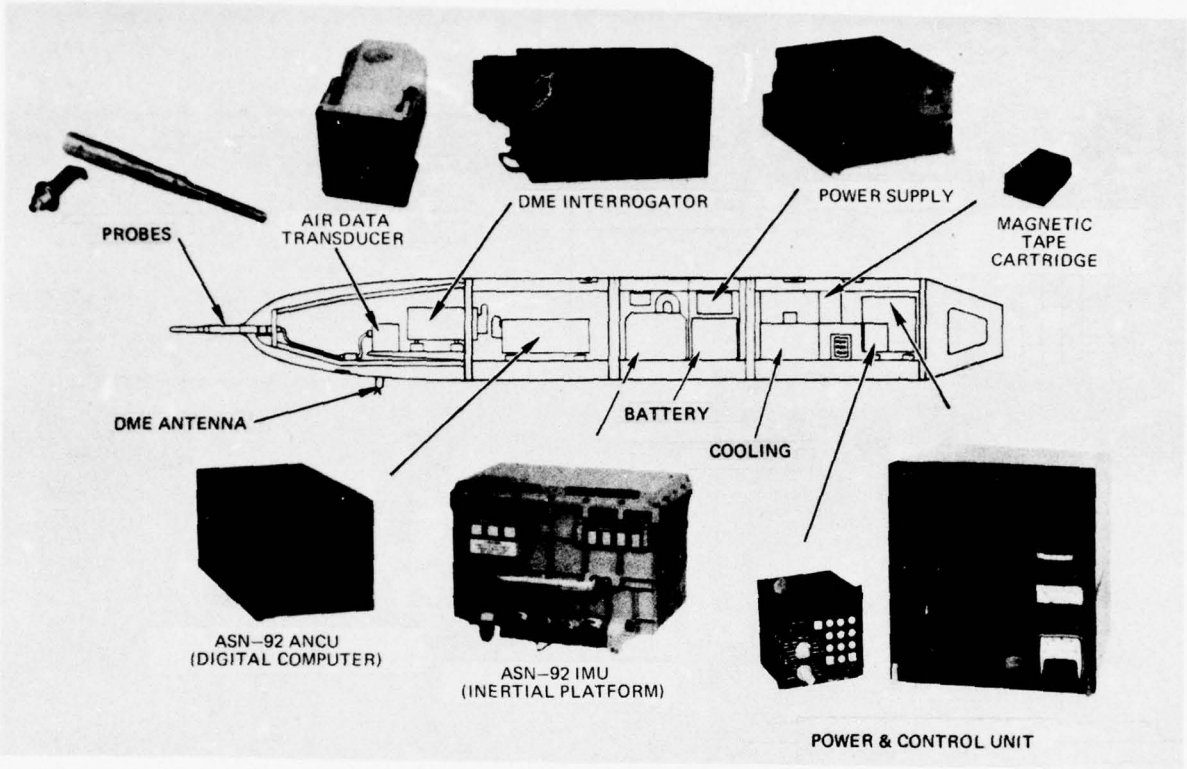

Figure 14. ARIS Airborne Pod

5.2.2 Operational Usage

To instrument a target for the ARIS, the transponders are located in the target area approximately as shown in figure 15. The central transponder should be located as close to the target as possible. All transponders should be placed to provide the clearest possible line of sight to the aircraft. The outer transponder positions must be surveyed accurately (to 1 foot) with respect to the central transponder (target). The approximate latitude and longitude coordinates of the central transponder are also required.

The pod operator composes the initialization data on the data terminal, records these data on the magnetic tape unit, and inserts this unit into the pod. The ground crew then transports

the pod to the aircraft and loads it onto the pylon station as they would handle and load a bomb. When the aircraft electrical power systems are energized (either by umbilical from the ground or by aircraft generated power), power appears at the weapon pylon station, automatically activating the pod subsystems and beginning inertial platform alignment. A flashing strobe light on top of the pod informs the aircrew that alignment is in progress. After about six minutes, alignment is complete and the strobe light goes out, signaling the pilot that the pod is in readiness for flight.

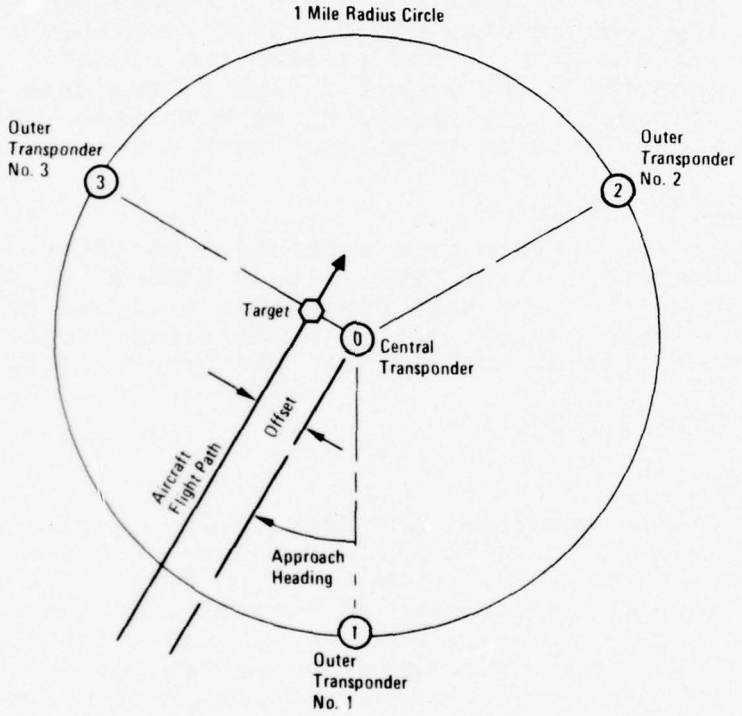

Figure 15. Standard ARIS Transponder Configuration

As the aircraft takes off and proceeds to the target area, the inertial navigation system (INS) in the pod monitors aircraft position. When the aircraft approaches within 10 miles of the target, the INS automatically commands the interrogator to commence interrogation of the transponder array. The interrogation data (range and range rate measurements) update inertial system position and velocity so that, when the aircraft reaches the simulated release point and transmits a release pulse to the pod, the pod can record aircraft position and velocity at release time accurately. These release conditions are refined

further or smoothed through transponder updates occurring after release in order to determine the release point to the greatest possible precision. This smoothing process continues until the aircraft is two miles beyond the target, when transponder updating ceases. The digital computer uses the smoothed release point data as initial conditions to solve the bomb trajectory equations and determine the impact point of the simulated bomb. The impact data are stored in computer memory as well as on magnetic tape for recovery by the pod operator after the mission.

After the aircraft returns to base and lands, the ground crew downloads the pod, and the pod operator removes the access door to the operator's station and removes the magnetic tape cartridge unit. He then takes the magnetic tape to the data terminal for print out of a hard copy record of each release recorded in flight. Figure 16 is an example of such a release record.

5.2.3 Release Record

Figure 16 is transcribed from a printout as obtained from a simulated bombing sortie. The release number (as indicated by the heading of the printout) shows that this was the second simulated release on the particular mission. Table VII gives the interpretation of the various data printed out.

5.3 FLIGHT TEST RESULTS

5.3.1 General

This subsection summarizes the results of a series of tests conducted in 1974 at Eglin Air Force Base, Florida to verify the performance of ARIS. From April to July of 1974, a joint Air Force/Navy team conducted an extensive series of flight tests to determine whether ARIS was suitable for subsequent use as the bomb scoring instrumentation system for the RABVAL program. The primary reference instrumentation for these tests was the Eglin AFB cinetheodolite range. Because, when at its best, ARIS achieves accuracies comparable to cinetheodolite accuracies, some missions employed a triad of extremely accurate ballistic cameras as the instrumentation system. Finally, actual bomb drops were made as an overall test of the ability of ARIS to predict actual impacts accurately.

5.3.2 Cinetheodolite-Referenced Tests

Figures 17 and 18 summarize the results of 337 separate simulated bombing runs conducted with ARIS being carried by either F111E or A6E aircraft. During these runs, the aircraft was being tracked by one of the cinetheodolite ranges at Eglin AFB. These figures display the CEP of the difference in impact

RELEASE - - NUMBER 2

COMP TIME AT RELEASE (SEC)	4558.635
(USEC)	326.75
DOWNRANGE MISS ERROR (FT)	268.2344
CROSSRANGE	63.65625
DOWNRANGE ESTIMATING ERROR (FT)	6.140625
CROSSRANGE	4
X TARGET COORDINATE (FT)	0
Y	0
Z	0
X IMPACT COORDINATE (FT)	−234.9844
Y	144.1875
SLANT RANGE TO IMPACT (FT)	6122.313
BOMB TRAIL (FT)	42.46875
TIME OF FALL (SEC)	6.546799
ALT. ERROR RANGE SENSITIVITY (FT/FT)	1.170039
VZ ERROR RANGE SENSITIVITY (FT/FT/SEC)	7.609375
X RELEASE COORDINATE (FT)	4635.591
Y	−1458.828
Z	3345.266
X VELOCITY AT RELEASE (FPS)	−754.5371
Y	246.531
Z	−403.6128
X REL POS STD DEV (FT)	2.680951
Y	3.6023
Z	4.295028
X REL VEL STD DEV (FT/SEC)	.1525333
Y	.2757298
BAROMETRIC ALTITUDE (FT)	6866.531
TRUE AIRSPEED (KTS)	496.6156
AIR TEMP (DEG K)	278.3881
AIR DENSITY (SLUGS/CU FT)	1.952494E−3
ANGLE−OF−ATTACK (DEG)	−3.823189
SIDESLIP (DEG)	.8456495
PITCH−ANGLE (DEG)	−28.94099
ROLL	−8.951197
HEADING	−73.85812
PITCH RATE (DEG/SEC)	.3896499
ROLL	1.487145
HEADING	−.4065156
PITCH AXIS LEVER ARM (RIGHT FT)	0
YAW (UP)	0
ROLL (FORWARD)	0
PITCH AXIS EJECTION VEL (RIGHT FT/SEC)	0
YAW (UP)	−7.5
ROLL (FORWARD)	0
EAST WIND VELOCITY	−48.12476
NORTH	−1.32373

Figure 16. Simulated Release Data Printout

TABLE VII. PRINTOUT INTERPRETATION

Entry	Interpretation
COMP TIME AT RELEASE (SEC) (USEC)	Time of release in seconds plus microseconds from computer turn-on prior to take-off: 4558.635327 seconds in this example
DOWNRANGE MISS ERROR (FT) CROSSRANGE	Bomb score in terms of downrange and crossrange miss distances as measured on a flat, horizontal plane through the target: 268 feet long; 64 feet to right of target in this example
DOWNRANGE ESTIMATING ERROR (FT) CROSSRANGE	The pod estimates its accuracy in computing the impact point, based on frequency and quality of transponder updates. These "estimating errors" represent the standard deviation of the miss errors: 6.1 feet and 4 feet in this example. The proper interpretation of the bomb scores and estimating errors is: "The downrange miss distance is 268 feet within a standard deviation of 6.1 feet; the cross-range miss distance is 64 feet within a standard deviation of 4 feet
X TARGET COORDINATE (FT) Y Z	The X, Y, and Z target coordinates are the northerly, easterly, and vertical offset distances of the target from the central transponder. In this example, the central transponder is on the target and the offsets are zero
X IMPACT COORDINATE (FT) Y	The X and Y impact coordinates are the northerly and easterly coordinates of the simulated bomb impact point with respect to the central transponder. They convey the same information as the downrange and crossrange miss errors, but in north-oriented rather than groundtrack-oriented coordinates
SLANT RANGE TO IMPACT (FT) BOMB TRAIL (FT) TIME OF FALL (SEC) ALT ERROR RANGE SENSITIV– ITY (FT/FT) VZ ERROR RANGE SENSITIVITY (FT/FT/SEC)	A summary of the results of the ballistic trajectory solution, including slantrange to impact (6122 feet), bomb trail (42.5 feet), time-of-fall (6.55 seconds), and the sensitivities of downrange impact errors to release altitude errors (1.17 ft/ft) and release vertical velocity errors 7.61 ft/ft/second)
X RELEASE COORDINATE (FT) Y Z X VELOCITY AT RELEASE (FPS) Y Z X REL POS STD DEV (FT) Y Z X REL VEL STD DEV (FT/SEC) Y	Release position and ground velocity and the standard deviation of these release conditions as estimated by the pod, based on the quality of transponder updating during the simulated bombing run. The standard deviation of the vertical (Z) component of release velocity is not listed since it is assumed, in the pod error model, to be a constant (0.316 feet per second)

TABLE VII. PRINTOUT INTERPRETATION (cont)

Entry	Interpretation
BAROMETRIC ALTITUDE (FT) TRUE AIRSPEED (KTS) AIR TEMP (DEG K) AIR DENSITY (SLUGS/CU FT) ANGLE-OF-ATTACK (DEG) SIDE SLIP (DEG)	Air data as computed at the release point. These are barometric altitude, true airspeed, air temperature, air density, angle of attack, and sideslip angle
PITCH ANGLE (DEG) ROLL HEADING	The aircraft attitude is recorded in terms of the pitch, roll, and true heading angles. This example shows the aircraft to have been in a 29-degree dive, with a 9-degree left roll, on a true heading of 286 degrees at release
PITCH RATE (DEG/SEC) ROLL HEADING	Attitude rate of the aircraft at release. In this example, the pitch rate was 0.4 degrees per second (pulling up), the roll rate was 1.5 degrees per second (rolling to the right), and the heading rate was -0.4 degrees per second (turning left)
PITCH AXIS LEVER ARM (RIGHT FT) YAW (UP) ROLL (FORWARD)	The three entries for lever arm (pitch, roll, and yaw) indicate the location of the bomb rack releasing the simulated bomb in relation to the bomb rack carrying the ARIS pod. In this example, the lever arms are zero, indicating that the bomb was released from the same pylon station which carried the pod.
PITCH AXIS EJECTION VEL (RIGHT FT/SEC) YAW (UP) ROLL (FORWARD)	The ejection velocity components simulated in the ballistic trajectory solution. This example shows a simulated bomb ejection velocity of -7.5 feet per second in a downward direction relative to the aircraft
EAST WIND VELOCITY NORTH	Wind components, in feet per second, as measured by the pod at aircraft altitude at release. In this example, the wind was primarily from the west at 48 feet per second

points as determined by differencing the aircraft release point state vectors measured by ARIS and by cinetheodolites, and propagating this difference theoretically into a ground plane impact error. In figure 17, these release point differences are propagated as if the simulated weapon were a low-drag (specifically a MK 84), 2000-pound bomb. In figure 18, the simulated weapon is a MK 82, 500-pound Snakeye retarded bomb. The demonstrated CEP for the simulated low-drag bomb releases (figure 17) was less than 15 feet in all cases except the high-speed (600-knot) runs, for which the CEP degraded to about 35

feet. The 15-foot accuracy figure held for all altitudes tested (500 to 10,000 feet), all speeds between 400 and 480 knots, and all delivery tactics employed (level, toss, pull-up, and break-away). For the high-drag simulated bomb releases (figure 18), the demonstrated CEP was less than 12 feet except for the extremely low altitude runs (200 feet above ground level) where a 500-foot or greater offset of the aircraft trajectory from the central transponder was used.

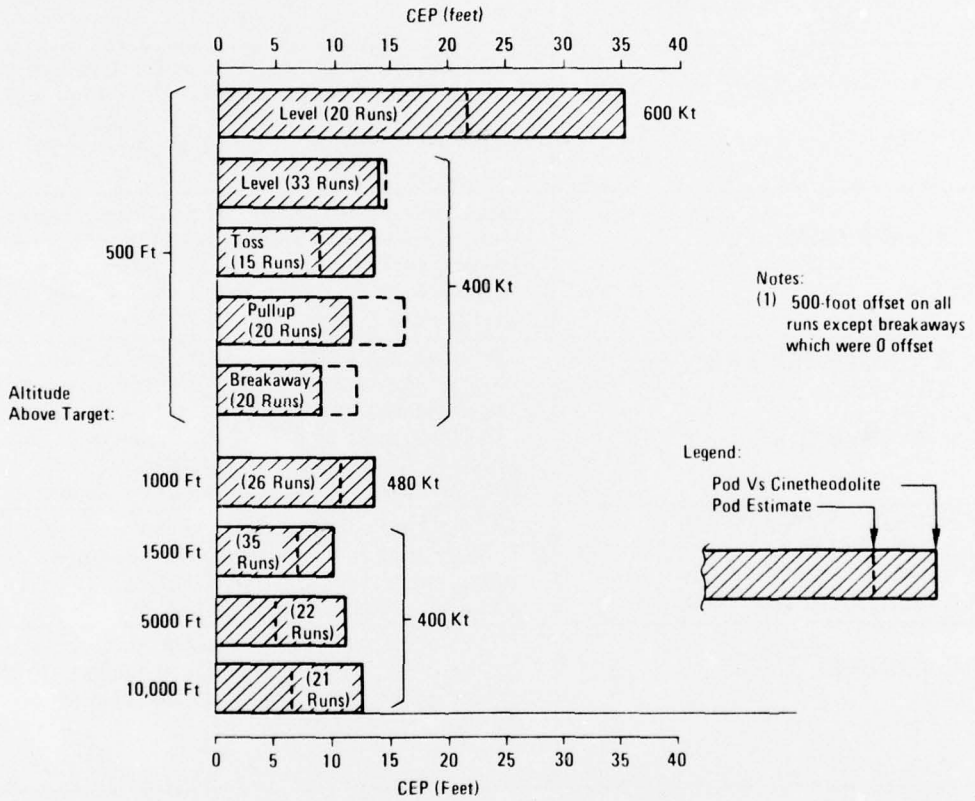

Figure 17. Simulated Low-Drag Bomb Release Test Results

Even the degraded accuracy figures indicate effective scoring because the aircraft has missed the target (central transponder) by at least 500 feet and ARIS scores that large miss to an accuracy an order of magnitude better than the actual miss distance. When the aircraft makes an accurate bombing run (i.e., zero offset), ARIS scores that run accurately as evidenced by the length of the topmost bar in figure 18.

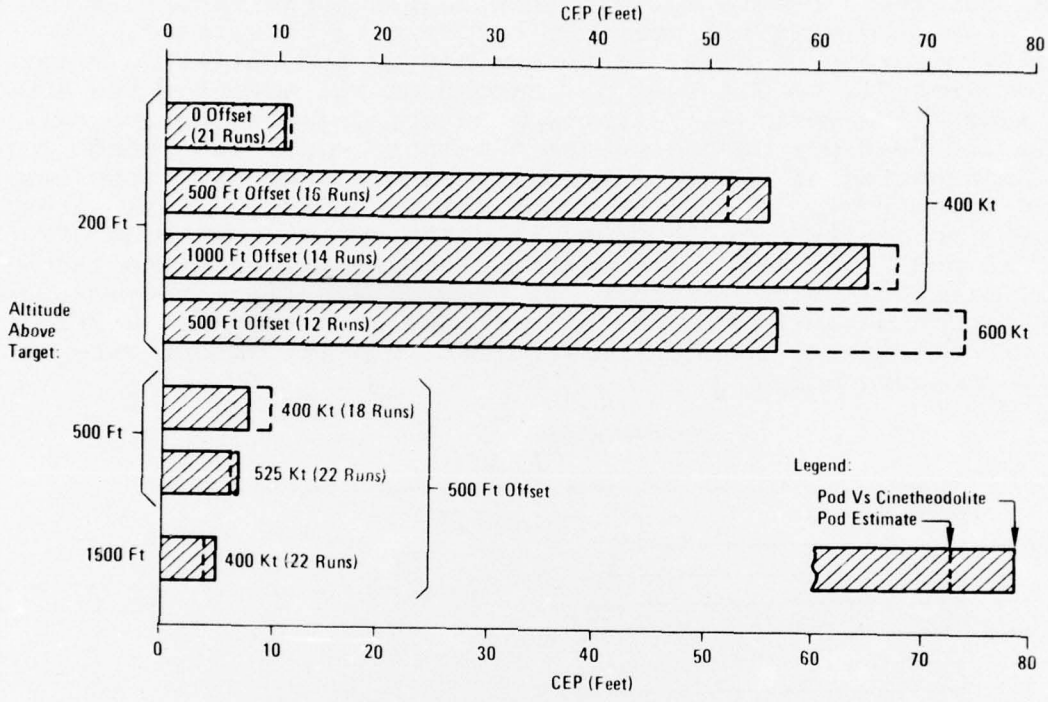

Figure 18. Simulated High-Drag Bomb Release Test Results

Each of the bars in the graphs of figures 17 and 18 is actually two bars; one (terminated by a solid line) representing the accuracy of ARIS as measured by the cinetheodolite range; the second (terminated by a broken line) representing the accuracy of ARIS as self-determined through its covariance matrix and impact error sensitivities. In most of the instances shown in these figures, the ARIS self-evaluation is in reasonably close agreement with the cinetheodolite-measured accuracy. Possible exceptions are the high-speed (600-knot) runs where the ARIS-estimated accuracy was optimistic by 15 or 20 feet for the low-drag results and pessimistic by the same amount in the high-drag case.

5.3.3 Ballistic Camera Referenced Tests

A few simulated bombing passes during the series of ARIS tests at Eglin AFB were instrumented with a triad of ballistic cameras. A total of 19 such passes yielded valid data. Of tese, 13 were at 400 knots; the remaining six, at 600 knots. Figure 19 shows the accuracy which ARIS achieved on these passes as determined

by the ballistic camera network (horizontal position errors of 1 to 3 feet and vertical position errors of 3 to 5 feet). The velocity accuracy of ARIS, as determined by the ballistic camera complex, was 0.2 to 0.4 feet per second on all axes for the 400-knot runs. The vertical velocity accuracy degraded to approximately 1.8 feet per second on the 600-knot runs. The reason for this degradation of vertical velocity accuracy at 600 knots was traced to excessive static pressure noise caused by shock waves sweeping across the static pressure ports on the nose boom of the ARIS pod. The ARIS uses static pressure to calculate barometric altitude which, in turn, is used to stabilize the vertical inertial channel. Litton has since redesigned the ARIS vertical channel software to reduce the vertical velocity sensitivity to static pressure noise.

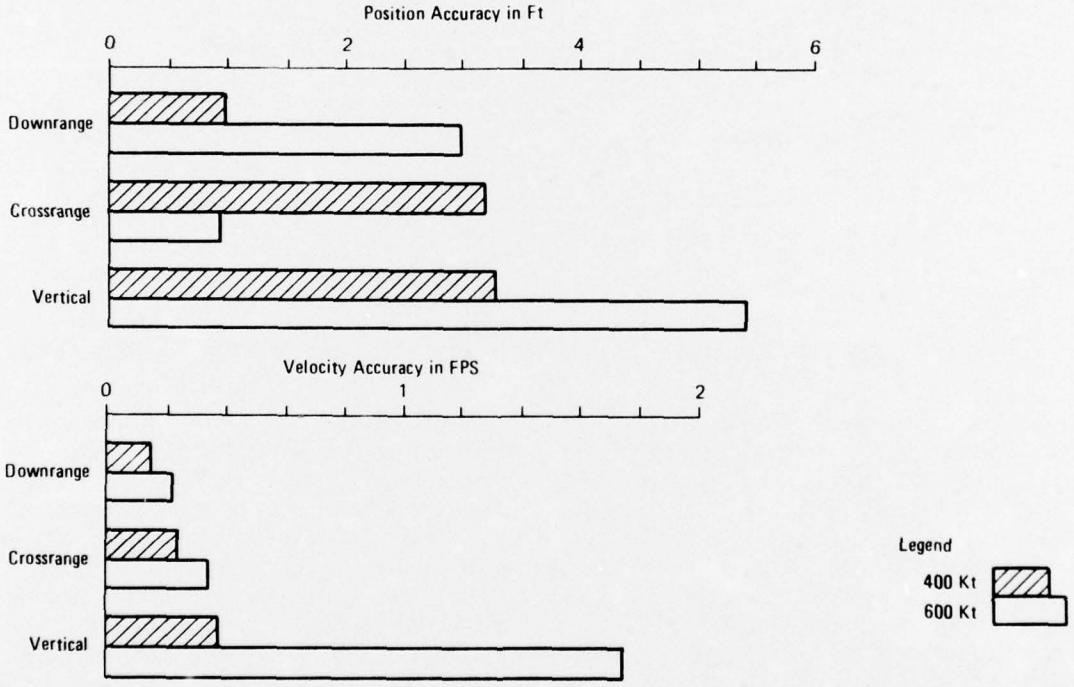

Figure 19. Ballistic Camera Measurements of ARIS Accuracy

5.3.4 Bomb Impact Tests

As final proof of the ability of ARIS to predict bomb impacts accurately, twenty-two MK 84, 2000-pound, low-drag bombs were actually released from F111E and A6E aircraft during the ARIS series of tests at Eglin AFB. Figure 20 shows the actual impacts (dots) with relation to the impact point (0,0) predicted by ARIS.

These drops demonstrated that ARIS could predict actual bomb impacts to an accuracy (CEP) of 21 feet. For the release conditions of these bomb drops, the prediction accuracy capability of ARIS, based on release position and velocity errors alone, is about 10 feet (CEP) as shown in figure 17. The growth in CEP from 10 to 21 feet is due to the accumulative effects of additional uncertainties in ejection velocity, separation disturbances (ballistic dispersion), and ballistic drag, as well as additional errors in measuring attitude, attitude rate, true airspeed, yaw sideslip angle, and air density.

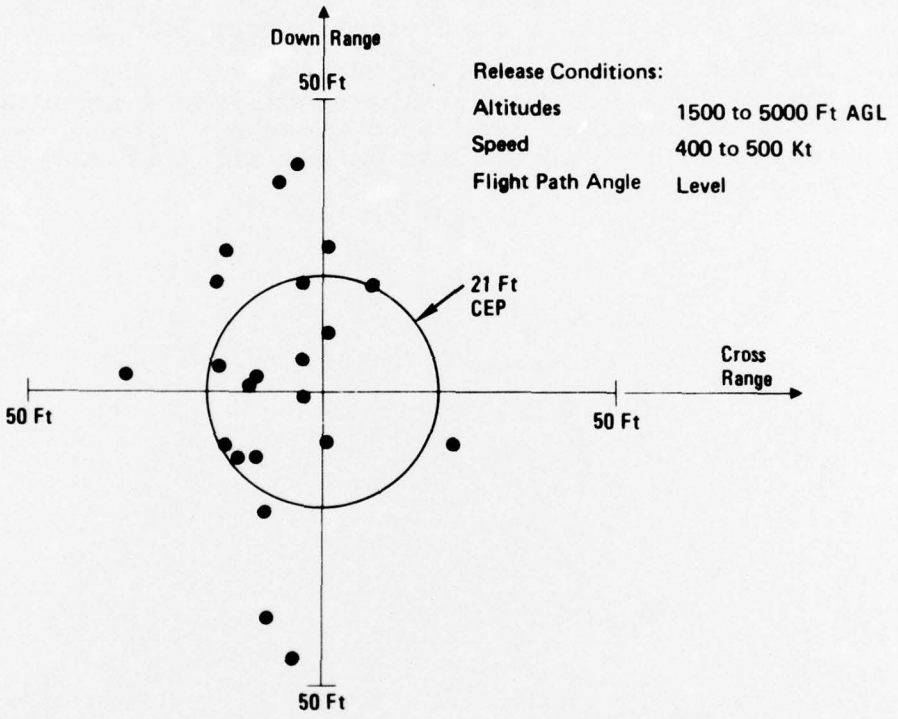

Figure 20. MK 84 Impacts vs ARIS Predictions

5.4 CONCLUSIONS

Based on the results of the ARIS flight tests conducted at Eglin Air Force Base in 1974, the following conclusions may be drawn:

a. The bomb scoring accuracy of ARIS (based on the accuracy of measuring the aircraft state vector at release) is better than 15 feet CEP with two exceptions:

(1) Extremely low altitude (200 feet) deliveries with large offsets (500 feet or more) of aircraft ground track relative to the central transponder.

(2) Very high speed deliveries (600 knots).

b. The ARIS predicted actual MK 84 bomb impacts, including uncertainties in ejection velocity, separation disturbances, and ballistics (as well as attitude and air data measurement errors) to an accuracy of 21 feet CEP.

c. The ARIS self-evaluation of its own accuracy is valid under all delivery conditions except 600 knots.

d. The ARIS satisfies all of the mobility, delivery mode, and operational versatility requirements necessary to score all-weather simulated attacks properly, employing realistic tactics against unfamiliar (off-range) targets.

SECTION VI

NDWS COST CONSIDERATIONS

6.1 GENERAL

Attempts to quantify the beneficial aspects of a scoring system in terms of cost savings necessarily involve some subjective judgements. Weapon delivery training is certainly essential. The only question is whether the quality of the training achieved justifies its expense. The compromises between the desired quality of training, the affordable cost, and the technological feasibility compel a careful consideration of the benefits derived, as well as the costs of the new equipments, in order to select a particular NDWS configuration judiciously.

Theoretically, it is possible to compare the effectiveness of NDWS systems having different accuracies; (1) by calculating the training cost differentials necessary to achieve a uniform level of training with all systems, or (2) by calculating the combat cost differentials implied by different levels of training. This type of cost effectiveness analysis, however, is beyond the scope of the present study. Instead an attempt will be made to compare the relative costs of two different NDWS configurations of equivalent or nearly equivalent capabilities.

6.2 NDWS COST MODELS

The acquisition and operating costs associated with NDWS depend upon the number of range areas, the number of squadrons using a range, and the number of training sorties flown by each squadron. The following discussion defines a baseline scenario or model of ranges and sortie rates and other factors contributing to acquisition and operating costs.

A total of ten NDWS ranges world-wide will probably fulfill all currently envisioned Navy training requirements. Five of these would be in the CONUS (Fallon, Yuma, Boardman, Dare County, and Pinecastle); three would be in the Pacific (Hawaii, and two in the western Pacific); and two would be in the Mediterranean (one east and one west). Each of these range areas defines a general location around which many targets would be defined. The primary scoring facilities would be moved occasionally to maintain fresh, unfamiliar targets for each squadron as it rotates through that training area.

Based on operational experience gained at Oceana NAS while using ARIS to score A6E simulated bombing sorties, three airborne scoring pods are sufficient to support a squadron of 12 aircraft. Therefore, 120 scoring pods are the most which would be needed to score all 40 squadrons of Navy attack aircraft on all training ranges. An even dispersal of these pods throughout the 10 ranges would result in an average provisioning of 12 pods per range. This 12 pod per range figure represents a world-wide average. Because each of the CONUS ranges might handle more than the average of four squadrons per day, these ranges may require more than 12 pods. Similarly, the oversea ranges may need less than the 12 pod per range average. Nevertheless, the following acquisition cost comparisons are developed based on the average range requirement of 12 pods per range.

6.3 NDWS ACQUISITION COST COMPARISONS

This subsection contains a comparison of the relative costs of two different NDWS system concepts (radar-inertial and DME-inertial), each of which may be in two different configurations (pod-mounted or inboard). The inboard versions are presumed to interface digitally with existing aircraft inertial navigation and air data systems to provide the necessary airborne measurements. The pod-mounted versions would be applicable for those aircraft that either contain no inertial navigation system or have no space internally in which to mount the additional airborne NDWS elements. In either case, whether the airborne NDWS elements are pod-mounted or internally-mounted, it is assumed that they are readily removable. The airborne NDWS elements are installed on or in the aircraft preparatory to that aircraft beginning an NDWS sortie, and are removed at the end of the sortie.

Table VIII lists the cost breakdowns for both the radar-inertial and the DME-inertial NDWS systems. Table IX presents the cost of outfitting a single NDWS range. These acquisition costs per range are based on the average range needs of 12 airborne units. They also include 20 percent spares.

Figure 21 shows the effect on the bottom line figures in table IX if there are more or less than 12 airborne sets per range. In particular, it reveals that for the inboard configurations, the DME-inertial NDWS system is less costly than the radar-inertial NDWS system for any number of airborne sets per range less than 27. Similarly, the DME-inertial NDWS pod system is less expensive than the corresponding radar-inertial system for any number of pods per range less than 45. Figure 21 is especially relevant to a test and evaluation range. In that case, only one or two airborne instrumentation sets are needed, and the

TABLE VIII. NDWS EQUIPMENT COST ESTIMATES

Equipment	Radar-Inertial	DME-Inertial
Ground-Based		
Radar	$1500K	---
Digital Computer	30K	$ 20K
Data Link Terminal	20K	---
DME Transponders (4)	---	180K
Sub Total	$1550K	$200K
Airborne (Pod)		
Pod Structure, Cooling, Power	$ 15K	$ 15K
Air Data Probe and Transducers	25K	25K
Digital Computer	30K	40K
Inertial Platform	60K	60K
Data Link	20K	---
Radar Beacon	20K	---
DME Interrogator	---	60K
Sub Total	$ 170K	$200K
Airborne (Inboard)		
Interface Adapter	$ 20K	$ 20K
Data Link	20K	---
Radar Beacon	20K	---
Digital Computer	---	30K
DME Interrogator	---	60K
Sub Total	$ 60K	$110K

TABLE IX. ACQUISITION COST PER NDWS RANGE

Equipment	Radar-Inertial	DME-Inertial
Ground-Based		
1 Set	$1550K	$ 200K
Spares	310K	40K
Sub Total	$1860K	$ 240K
Airborne (Pod)		
12 Sets	$2040K	$2400K
Spares	408K	480K
Sub Total	$2448K	$2880K

TABLE IX. ACQUISITION COST PER NDWS RANGE (cont)

Equipment	Radar-Inertial	DME-Inertial
Airborne (Inboard)		
12 Sets	$ 720K	$1320K
Spares	144K	264K
Sub Total	$ 864K	$1584K
Total NDWS Cost Per Range		
(Pod)	$4,308K	$3,120K
(Inboard)	$2,724K	$1,824K

DME systems are markedly superior to the radar systems in terms of acquisition costs.

6.4 *OTHER COST CONSIDERATIONS*

The foregoing cost analysis does not include other cost factors which contribute to system life cycle cost. Other such costs which should be considered, but merit more careful treatment than the scope of this study permits, are development costs, land and base facility acquisition or rental costs, training costs for operating and maintenance personnel, aircraft modification and installation costs, and annual costs for operation and maintenance personnel as well as for replacement parts. A cursory qualitative discussion of these items as they affect the different NDWS configurations is still appropriate herein, even though a quantitative treatment is avoided.

Development costs will probably be roughly the same for all concepts. If anything, the radar approaches may tend to have the higher development costs in view of the high accuracy of the position data required. Land and base facility costs will undoubtedly be higher for the radar than for the DME because the radar equipment is much larger and less mobile.

Training costs tend to be proportional to the number of operating and maintenance personnel required. The personnel needed to operate and maintain the airborne elements will be the same for both the radar-inertial and DME-inertial. The major difference is in the number of ground equipment operators. The radar requires manning around the clock for 24-hour NDWS operations,

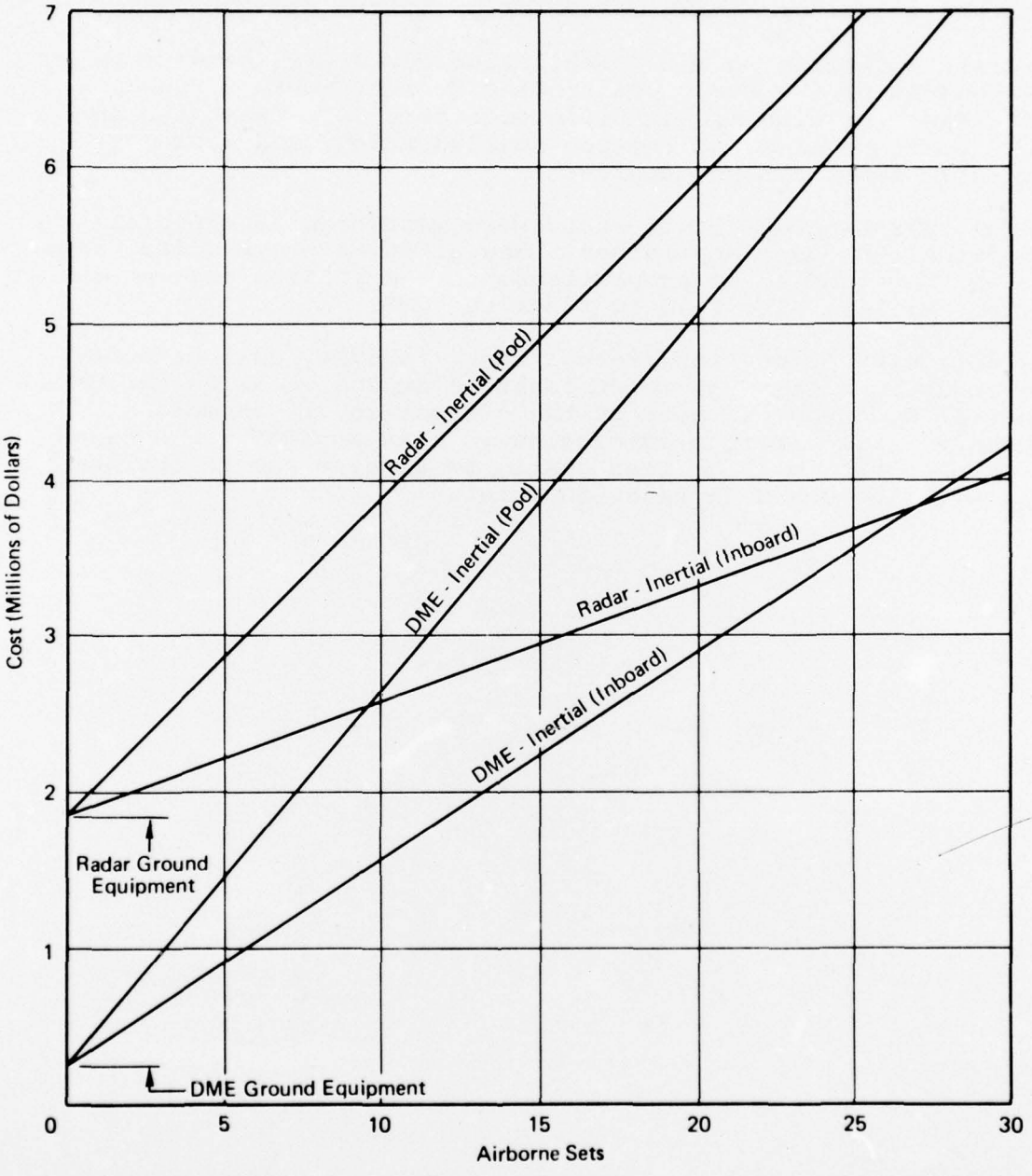

Figure 21. Comparative Acquisition Costs Per Range

while the DME transponders are virtually unattended. This cost advantage of the DME approach becomes amplified even further when the annual operating costs for personnel are included.

Aircraft modification and installation costs will tend to be independent of the basic positioning device, whether radar or DME. The most significant difference here is between the in-board configuration and the pod configuration, and will obviously favor the pod approach.

Annual operating personnel costs were mentioned as especially impacting the radar approaches. Annual maintenance costs, inso-far as they tend to be proportional to the initial cost of the equipment, will also tend to favor the DME.

The foregoing discussions reveal that, in every cost category, the radar-inertial NDWS is at least as expensive as is the DME-inertial NDWS and, in most of the categories, it is more expensive. The obvious conclusion is that an NDWS range based on DME-inertial will be less costly to acquire and to operate than will one based on radar-inertial.

SECTION VII
CONCLUSIONS

The major conclusions from each of the foregoing sections are summarized below.

a. Measurements of the aircraft states at the release point for no-drop bomb scoring should be at least as accurate as the following:

Position	20 ft (horizontal) 30 ft (vertical)
Velocity	2 fps (horizontal) 3 fps (vertical)
Heading	0.3 deg
Roll Rate	6 deg/sec
True Air Speed	5 fps
Air Pressure and Temperature	1 percent

b. To incorporate strafe scoring into NDWS, position measurement accuracy to within 3 feet and pitch and heading measurement accuracy to 0.1 degree would be required.

c. An NDWS implemented with airborne inertial platform data combined with either radar or DME position tracking data can comfortably satisfy the bomb scoring requirements and may even satisfy the strafe scoring requirements.

d. ARIS, an existing DME-inertial no-drop bomb scoring system, has demonstrated that it has the accuracy, mobility, and operational versatility to score properly all-weather no-drop bombing runs which employ realistic tactics against unfamiliar (off-range) targets.

e. A DME-inertial NDWS range will be less costly to acquire, maintain, and operate than will a radar-inertial NDWS of equivalent accuracy.

REFERENCES

1. "Operational Test and Evaluation of Tactical Radar Bombing Systems - Results of Demonstration Test of a Bomb Scoring System", WSEG Report 253, November, 1974.

2. "Theoretical Analysis and Experimental Measurements of Separation Disturbances in Weapon Delivery Systems", J.S. Ausman JTCG/MD WP No. 12 Aircraft/Stores Compatibility Symposium Proceedings, 2 - 4 September 1975.

3. "A Ballistic Trajectory Algorithm for Digital Airborne Fire Control," Naval Weapons Center, China Lake, Report No. NWC TP 5416, September, 1972.

4. "A Stretch Computer Program for Integration of Two-Dimensional Trajectories," Naval Surface Weapons Center, Dahlgren, Va. Technical Memorandum No. K-8/65.